

1 **Noble gas and carbon isotope systematics at the seemingly inactive Ciomadul**
2 **volcano (Eastern-Central Europe, Romania): evidence for volcanic degassing**
3

4 **B. M. Kis^{1,2,3*}, A. Caracausi⁴, L. Palcsu³, C. Baci⁵, A. Ionescu^{5,1}, I. Futó³, A. Sciarra⁶, Sz.**
5 **Harangi^{1,7}**

6 1. MTA-ELTE Volcanology Research Group, H-1117 Budapest, Pázmány sétány 1/C, Hungary,
7 szabolcs.harangi@geology.elte.hu

8 2. Babes-Bolyai University, Faculty of Biology and Geology, Kogalniceanu 1, Romania,
9 kis.boglarka@ubbcluj.ro

10 3. Isotope Climatology and Environmental Research Centre, Institute for Nuclear Research,
11 Hungarian Academy of Sciences, H-4026 Debrecen, Bem tér 18/C, Hungary,
12 palcsu.laszlo@atomki.mta.hu, futo.istvan@atomki.mta.hu

13 4. Istituto Nazionale di Geofisica e Vulcanologia, Sezione Palermo, IT-90146 Palermo, Via Ugo
14 La Malfa 153, Italy, antonio.caracausi@ingv.it;

15 5. Babes-Bolyai University, Faculty of Environmental Science and Engineering, RO-400294
16 Cluj-Napoca, Fântânele 30, Romania, artur.ionescu@ubbcluj.ro, calin.baciu@ubbcluj.ro

17 6. Istituto Nazionale di Geofisica e Vulcanologia, Sezione Roma 1, IT-00143 Roma, Via V.
18 Murata 605, Italy, alessandra.sciarra@ingv.it

19 7. Department of Petrology and Geochemistry, Eötvös Loránd University, Budapest, Hungary

20 Corresponding author: B.M. Kis (kis.boglarka@ubbcluj.ro, kisboglarka85@gmail.com)

21 **Key Points:**

- 22 • CO₂ emissions at Ciomadul, Eastern-Central Europe, suggest a still-active plumbing
23 system beneath the volcano in spite of long dormancy.
- 24 • The CO₂ and He isotope compositions provide evidence for significant contribution of
25 magma-derived volatiles, up to 80%.
- 26 • Isotopic signatures of gases indicate that primary magmas could have derived from a
27 mantle source modified by subduction-related fluids.

28

29 **Abstract**

30

31 Ciomadul is the youngest volcano in the Carpathian-Pannonian Region, Eastern-Central Europe,
32 which last erupted 30 ka. This volcano is considered to be inactive, however, combined evidence
33 from petrologic and magnetotelluric data, as well as seismic tomography studies suggest the
34 existence of a subvolcanic crystal mush with variable melt content. The volcanic area is
35 characterized by high CO₂ gas output rate, with a minimum of $8.7 \times 10^3 \text{ t yr}^{-1}$. We investigated
36 31 gas emissions at Ciomadul to constrain the origin of the volatiles. The $\delta^{13}\text{C-CO}_2$ and $^3\text{He}/^4\text{He}$
37 compositions suggest the outgassing of a significant component of mantle-derived fluids. The He
38 isotope signature in the outgassing fluids (up to 3.10 R_a) is lower than the values in the peridotite
39 xenoliths of the nearby alkaline basalt volcanic field (R/R_a 5.95R_a±0.01) which are
40 representative of a continental lithospheric mantle and significantly lower than MORB values.
41 Considering the chemical characteristics of the Ciomadul dacite, including trace element and Sr-
42 Nd and O isotope compositions, an upper crustal contamination is less probable, whereas the
43 primary magmas could have been derived from an enriched mantle source. The low He isotopic
44 ratios could indicate a strongly metasomatized mantle lithosphere. This could be due to
45 infiltration of subduction-related fluids and postmetasomatic ingrowth of radiogenic He. The
46 metasomatic fluids are inferred to have contained subducted carbonate material resulting in a
47 heavier carbon isotope composition ($\delta^{13}\text{C}$ is in the range of -1.4 to -4.6 ‰) and an increase of
48 CO₂/³He ratio. Our study shows the magmatic contribution to the emitted gases.

49

50 **Plain Language Summary**

51

52 Determining the fluxes and composition of gases in active and dormant volcanoes could help to
53 constrain their origin. Ciomadul is the youngest volcano of the Carpathian-Pannonian Region,
54 Eastern-Central Europe, where the last eruption occurred 30 ka. Its eruption chronology is
55 punctuated by long quiescence periods (even >100 kyrs) separating the active phases; therefore,
56 the long dormancy since the last eruption (30 ka) does not unambiguously indicate inactivity.
57 Knowing if melt-bearing magma resides in the crust is fundamental to evaluate the nature of the
58 volcano. Isotopic compositions of helium ($^3\text{He}/^4\text{He}$) and carbon ($\delta^{13}\text{C}_{\text{CO}_2}$) are important tools for
59 the study of the origin of the gases. We show that the isotope variation of the emitted gases
60 suggests a metasomatized lithospheric mantle origin for the primary magmas. This is consistent
61 with a degassing deep magma body existing beneath Ciomadul and that this long-dormant
62 volcano cannot be considered as extinct.

63 **1. Introduction**

64

65 Gas emissions are often associated with active or dormant volcanic areas and regions
66 affected by extensional tectonics (e.g., O'Nions & Oxburgh, 1988, Oppenheimer et al., 2014).
67 Monitoring of fluids (chemical and isotopic compositions and physical properties) in volcanic
68 regions provides important information concerning the processes occurring at depth (e.g.,
69 Edmonds, 2008; Fischer, 2008; Christopher et al., 2010; Mazot et al., 2011; Ruzié et al., 2012;
70 Agosto et al., 2013; Barry et al., 2013, 2014; Caliro et al., 2015; Roulleau et al., 2016; Tassi et
71 al., 2010, 2011, 2016; Wei et al., 2016). The chemical and isotopic composition of the emitted

72 fluids in active volcanoes is primarily controlled by magmatic processes, such as the injection of
73 new magma into the plumbing system or degassing of deep mafic magma in the lower crust, or
74 interaction with the volcanic hydrothermal systems, among others (e.g., Caracausi et al., 2003,
75 2013; Edmonds, 2008; Christopher et al., 2010; Paonita et al., 2012, 2016; Sano et al., 2015).
76 Furthermore, compositional change of the fluids may also correlate with the seismicity at
77 regional scale (e.g., Chiodini et al., 2004; Bräuer et al., 2008; 2018; Melián et al., 2012,
78 Cardellini et al., 2017).

79 There has been major progress in understanding the factors controlling gas emissions in
80 active and dormant volcanic areas during the last two decades (Aiuppa et al., 2007; Edmonds,
81 2008; Oppenheimer et al., 2014; Lee et al., 2016; Moussallam et al., 2018); however, much less
82 attention has been given to seemingly inactive volcanic areas (Rouilleau et al., 2015). These are
83 volcanoes that last erupted more than 10 ka and at the surface there are no signs of reawakening.
84 The Tatun volcanic complex in Taiwan is an example of such a volcanic system. Although the
85 last eruption occurred 20 ka, geophysical data indicates a still-active magma storage. The
86 composition of emitted gases is consistent with this interpretation, as they contain significant
87 magmatic components (Rouilleau et al., 2015). The importance and the potential hazard of such
88 volcanoes are shown by the case of the Ontake volcano in Japan. There were no proven records
89 of historical and even Holocene eruptions before the phreatic eruptive event in 1979 and
90 therefore, there were no detailed studies and monitoring on this volcano. In 2014, another
91 phreatic eruption occurred, causing serious fatalities (Kato et al., 2015) and pointed to the
92 requirement to better understand such long-dormant volcanoes. Sano et al., (2015) demonstrated
93 that regular monitoring of volcanic gases is fundamental to understand the behaviour of these
94 apparently inactive volcanoes. In this regard, detection of a magmatic chamber containing some
95 melt fraction could mean the potential for reactivation even after several tens of kyrs dormancy.
96 Emission of gases with isotopic signatures in the range of magmatic values can be evidence of
97 magma intrusions at depth (Farrar et al., 1995; Sorey et al., 1998; Pizzino et al., 2002; Carapezza
98 et al., 2003, 2012; Carapezza & Tarchini, 2007; Bräuer et al., 2008; 2018; Caracausi et al., 2013,
99 2015; Fischer et al., 2014; Rouwet et al., 2014, 2017; Sano et al., 2015), in addition to
100 recognition of geophysical anomalies reflecting melt pockets at depth (Comeau et al., 2015;
101 2016; Harangi et al., 2015a).

102 Ciomadul is the youngest volcano within the Carpathian-Pannonian Region, Eastern-
103 Central Europe, where the last eruption occurred 30 ka (Harangi et al., 2010; 2015b; Molnár et
104 al., 2019). Thus, it is usually considered as an inactive volcano. In spite of its long dormancy,
105 combined evidence from petrologic and magnetotelluric data (Kiss et al., 2014; Harangi et al.,
106 2015a), as well as seismic tomography (Popa et al., 2012) suggest the presence of a melt-bearing
107 crystal mush beneath the volcano. This is consistent with the local high heat flow (85-120
108 mW/m²) compared to the Carpathian Range where this value decreases to 40-60 mW/m²
109 (Demetrescu & Andreescu, 1994, Horváth et al., 2006), the high flux of carbon-dioxide of $8.7 \times$
110 10^3 t yr⁻¹ (Kis et al., 2017) the presence of mineral and thermal waters up to 78°C (Jánosi, 1980;
111 Rădulescu et al., 1981) and the geodynamically active region (Wenzel et al., 1999; Ismail-Zadeh
112 et al., 2012). The eruption chronology of the Ciomadul lava dome field (Molnár et al., 2018) is
113 characterized by prolonged quiescence periods between the active phases, often exceeding 100
114 kyrs.

115 There are a number of sites at Ciomadul, where significant amount of CO₂ gases are
116 emitted (Kis et al., 2017). Althaus et al. (2000), Vaselli et al. (2002), Frunzeti (2013) and Sarbu et
117 al (2018) studied the composition of gases collected from a few locations and concluded that

118 they could indicate a deep-seated magma body below the volcano. Here, we present a
119 comprehensive helium isotope signature (hereafter $^3\text{He}/^4\text{He}$) and carbon isotope (hereafter
120 $\delta^{13}\text{C}_{\text{CO}_2}$) systematics of the volatile degassing from Ciomadul based on a detailed sampling of all
121 the main known locations of gas emissions to constrain the origin of fluids and to characterize
122 the nature of a seemingly inactive volcano.

123 124 **2. Geological setting**

125 126 **2.1. Ciomadul Volcanic Dome Field**

127
128 Ciomadul volcano is located at the southeastern edge of the Carpathian-Pannonian
129 Region, at the southern end of the Călimani-Gurghiu-Harghita volcanic chain (Szakács et al.,
130 1993, Szakács & Seghedi, 1995; Pécskay et al., 2006; **Figure 1**). It is part of a post-collisional
131 volcanic belt, which comprises a series of andesitic to dacitic volcanoes, developed parallel with
132 the Carpathian orogeny. The volcanism occurred well after the continent-continent collision
133 between the Tisza-Dacia microplate and the western margin of the Eurasian plate (Csontos et al.,
134 1992; Matenco and Bertotti 2000, Cloetingh et al, 2004; Seghedi et al., 2004; 2005; 2011;
135 Matenco et al, 2007). Ciomadul is part of a lava dome field and this central volcanic complex
136 involves 8-14 km³ of high-K dacitic lavas (Karátson & Timár, 2005, Szakács et al, 2015; Molnár
137 et al., 2019). The volcano developed on the Early Cretaceous clastic flysch sedimentary unit of
138 the Eastern Carpathians that forms several nappes. It consists of binary alternation of sandstones,
139 calcareous sandstones, limestones and clays/marls from the Sinaia Formation of the Ceahlau
140 nappe and the Bodoc flysch (Băncilă, 1958; Ianovici & Radulescu, 1968; Nicolăescu, 1973;
141 Grasu et al., 1996). The flysch unit has a thickness up to 2500 m.

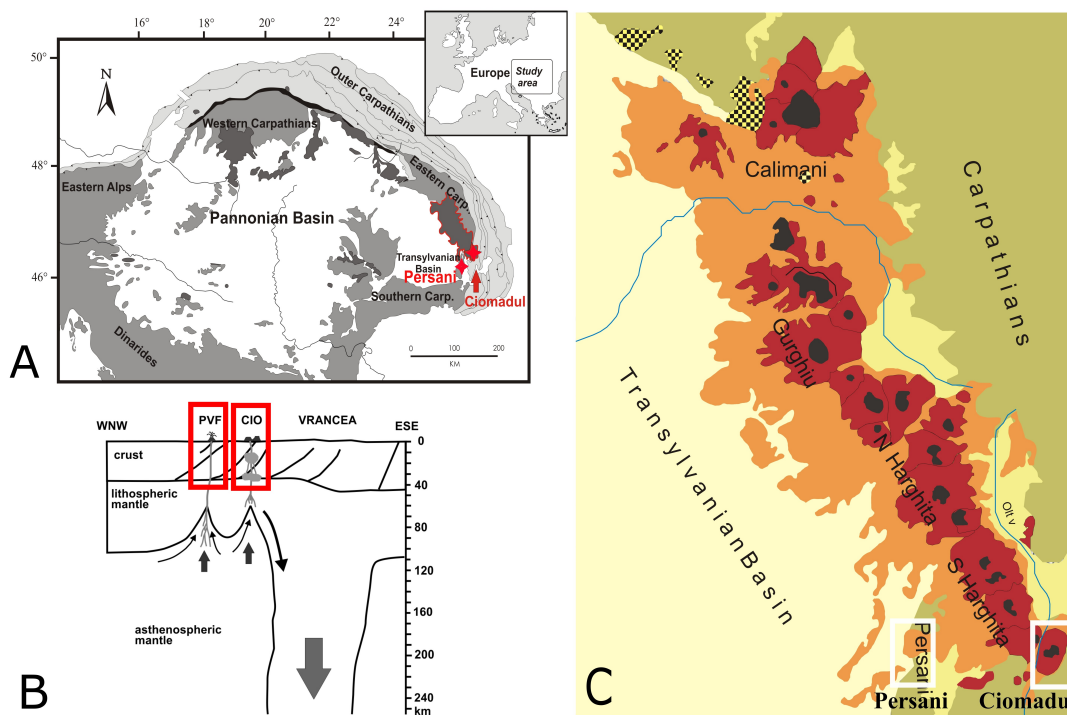
142 The Ciomadul volcanic complex is made up by amalgamation of several lava domes
143 truncated by two explosion craters called Mohos and Saint Anna (Szakács et al., 2015). This
144 central volcano is surrounded by further isolated lava domes (Baba Laposă, Haramul Mic, Dealul
145 Mare, Būdös-Puturosul and Bálványos; Molnár et al., 2018, **Figure 2**). Volcanism at the
146 Ciomadul volcanic dome field started around 1 Ma, while the most voluminous Ciomadul
147 volcanic structure has developed over the last ca. 160 kyr (Molnár et al., 2018; 2019). During the
148 first volcanic stage, the intermittent lava dome extrusions were separated by relatively long
149 dormant periods even exceeding 100 kyr. The second volcanic stage was characterized by initial
150 lava dome effusion and then, after ca. 40 kyrs of quiescence, a more explosive volcanic activity
151 occurred (from 57 to 30ka, Moriya et al, 1995, 1996; Vinkler et al, 2007; Harangi et al., 2010,
152 2015b; Karátson et al., 2016; Molnár et al., 2018; 2019). This stage involved lava-dome collapse
153 events, vulcanian and sub-plinian to plinian explosive eruptions (Vinkler et al, 2007; Harangi et
154 al., 2015b; Karátson et al., 2016). The eruptive products are relatively homogeneous K-rich
155 dacites (Szakács and Seghedi, 1987; Szakács et al., 1993; Vinkler et al., 2007; Molnár et al.,
156 2018; 2019). Petrogenetic and thermobarometric studies on amphiboles as well as combined U-
157 Th/He and U/Th zircon dating suggest the presence of a long-lasting (up to 350 kyrs) crystal
158 mush body in the crust. This appears to be mostly at relatively low-temperature just above the
159 solidus (700-750°C) and is periodically partly remobilized by injections of fresh basaltic magmas
160 that could rapidly trigger volcanic eruptions (Kiss et al., 2014; Harangi et al., 2015a; 2015b).

161 The Ciomadul volcano is located near (~50 km) the Vrancea seismic region (Wenzel et
162 al., 1999; Ismail-Zadeh et al., 2012) located at the arc bend between the Eastern and the Southern
163 Carpathians. Frequently occurring earthquakes have deep hypocentres (70-170 km) delineating a

164 narrow, vertical region. This is consistent with a high-velocity seismic anomaly interpreted as a
 165 cold lithosphere slab descending slowly into the asthenospheric mantle (Wortel & Spakman,
 166 2000). Further crustal and subcrustal earthquakes ($M < 4$) occur occasionally around the Perșani
 167 basalt volcanic field and the Ciomadul volcano (Popa et al., 2012). The seismic tomographic
 168 model indicates a vertically-extended low-velocity anomaly beneath Ciomadul. This can be
 169 interpreted as trans-crustal magma storage with an upper melt-dominated magma chamber (Popa
 170 et al., 2012). The seismic tomographic model is supported by the result of combined petrologic
 171 and magnetotelluric studies which demonstrated the existence of a low-resistivity anomaly and
 172 the depth of 5-20 km beneath the volcanic centers of Ciomadul, inferred to be a melt-bearing
 173 crystal mush (Harangi et al., 2015a). In addition, a deeper low-resistivity anomaly was also
 174 detected at a depth of 30-40 km, possibly related to a deeper magma accumulation zone at the
 175 crust-mantle boundary.

176 Another Pleistocene monogenetic basalt volcanic field is approximately 40 km from the
 177 Ciomadul, at the southeastern part of the Carpathian–Pannonian Region (Figure 1), at the
 178 boundary between the Perșani Mts. and the Transylvanian basin (Seghedi & Szakács, 1994;
 179 Downes et al., 1995; Harangi et al., 2013; Seghedi et al., 2016). Basaltic volcanism occurred here
 180 between 1.14 Ma and 683 ka (Panaiotu et al., 2004, 2013) and formed several volcanic centers
 181 accompanied by maars, scoriacones and lava flows. The erupted basaltic magma carried
 182 significant amount of ultramafic xenoliths from the lithospheric mantle (peridotites and
 183 amphibole pyroxenites) revealing the nature of the uppermost mantle of this region (Vaselli et
 184 al., 1995; Falus et al., 2008).

185
 186



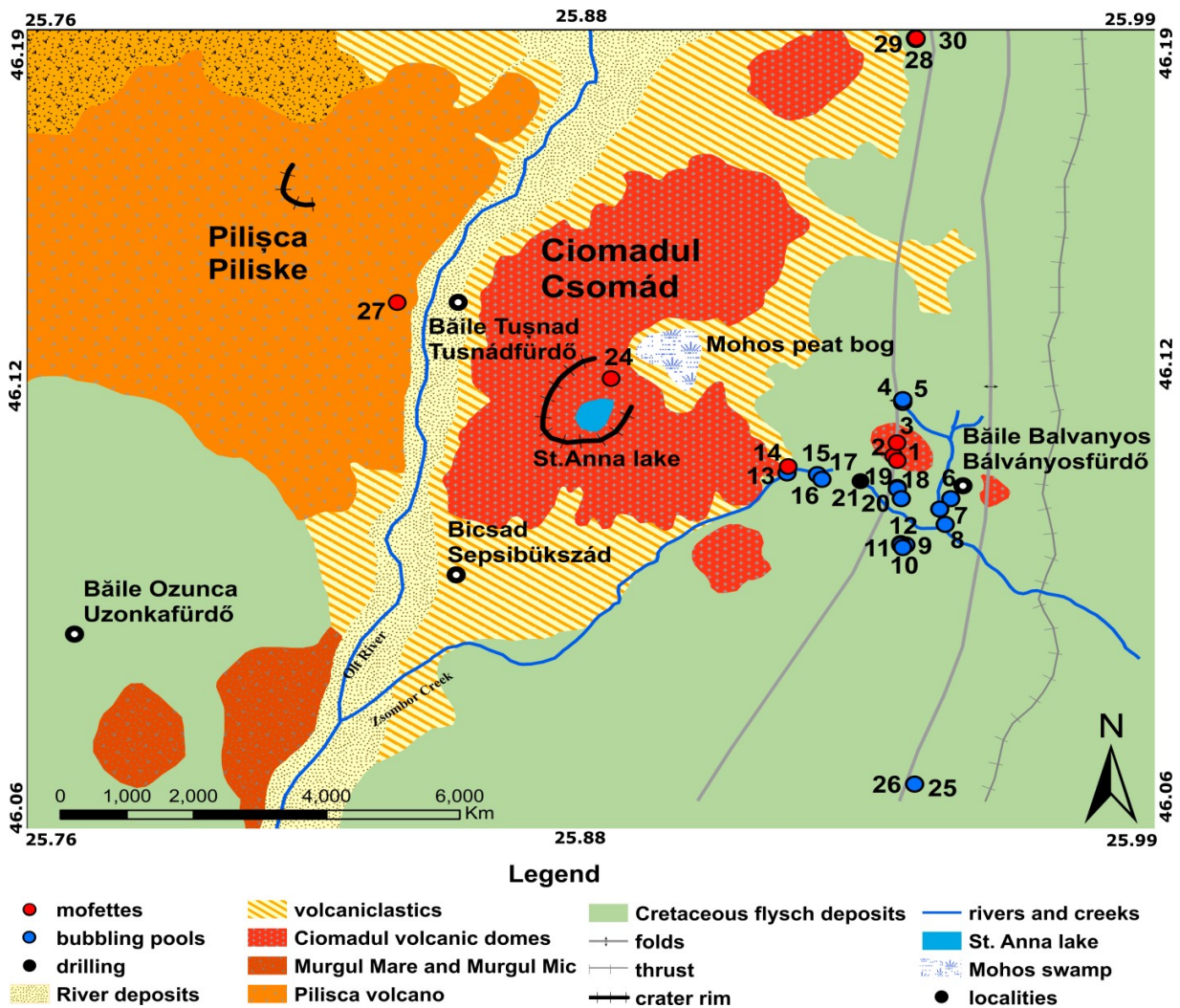
187
 188

189 **Figure 1a:** Location of Ciomadul and Persani volcanoes in the southeastern Carpathian area of the Carpathian-
 190 Pannonian Region (after Harangi et al., 2013), **1b:** Geotectonic model of the Persani and Ciomadul volcanic areas,
 191 PVF=Persani Volcanic Field, CIO=Ciomadul (after Harangi et al., 2013), **1c:** Location of Ciomadul and Persani
 192 volcanoes in the volcanic range of the Eastern Carpathians (modified after Szakács & Seghedi, 1995)

193
194
195
196
197
198
199
200
201
202
203

2.2 Gas emissions and mineral water springs at Ciomadul volcanic area

Gas emanations in the form of bubbling pools and low-temperature (T~8-10°C) dry mofettes are characteristic of the Ciomadul volcano. CO₂-bubbling peat bogs can be also found, mainly at the north-eastern (Buffogó peat bog) and southern parts of the Puturosul Mts. (Zsombor-Valley, Jánosi et al., 2011). The minimum total CO₂ flux was estimated to be $8.7 \times 10^3 \text{ t yr}^{-1}$ (Kis et al., 2017). The aquifers of this area are represented by CO₂-rich sparkling mineral water, with temperature up to 22.5 °C (Berszán et al., 2009; Jánosi et al., 2011; Italiano et al., 2017).



204
205
206
207
208
209
210
211

Figure 2: Geological sketch map of the study area. The red, black and blue dots indicate the type of the sampling points: mofette, drilling and bubbling pool respectively. The numbers on the sampling sites are the same as in Tables 1. (Geological map is modified after Ianovici & Radulescu, 1968)

3. Sampling and analytical methods

212 A total of 31 sites were selected for this study, including bubbling pools, dry gas
213 emissions (mofettes) and one drilling (**Figure 2 and Table 1**). We collected fluids during two
214 field campaigns carried out in the spring and autumn of 2016 respectively. In the 1st field
215 campaign, gas samples were collected for $\delta^{13}\text{C-CO}_2$ and $^3\text{He}/^4\text{He}$ composition in 1l evacuated
216 Pyrex glass tubes with a vacuum stop-cock, while for chemical composition, gas samples were
217 collected in 150 ml glass tubes with two vacuum stop-cocks. Chemical compositions were
218 analyzed at the Istituto Nazionale di Geofisica e Vulcanologia, Rome, Italy, whereas chemical
219 and isotopic composition of water, noble gas compositions (He, Ne) and $\delta^{13}\text{C-CO}_2$ of gas
220 samples were measured at the Isotope Climatology and Environmental Research Centre (ICER),
221 Institute for Nuclear Research, Hungarian Academy of Sciences, Debrecen, Hungary. During the
222 2nd field campaign, the samples were collected in glass and steel samplers equipped with two
223 valves. These samples were analyzed for their elemental composition (He, Ne, Ar, H₂, O₂, N₂,
224 CO, CH₄ and CO₂), $\delta^{13}\text{C}$ (CO₂), $^3\text{He}/^4\text{He}$ ratios and, ^{20}Ne abundances at the Istituto Nazionale di
225 Geofisica e Vulcanologia, Palermo, Italy.

226 We also separated clinopyroxene mineral grains (> 3 g in weight) from one of the
227 ilherzolite xenoliths collected at the foot of the Gruiu scoria cone, in the Perşani volcanic field.
228 The noble gas composition of the fluid inclusions were analysed at Istituto Nazionale di
229 Geofisica e Vulcanologia, Palermo, Italy.

230

231 Table 1.

232 *List of the sites investigated including location names, geographical position (geographical coordinates in WGS84),*
233 *type of manifestation (mofetta, bubbling pool, drilling), type of sample (free gas) and field data (temperature, pH*
234 *and EC-expressed in $\mu\text{S}/\text{cm}$) where available.*

235 *Note. nd=not determined.*

236

237

238 **3.1 Chemical and isotopic composition of gases**

239

240 The chemical composition of the samples from the 1st campaign was analysed with a
241 Portable Varian CP4900 Micro Gas Chromatograph. This Micro GC is configured for the
242 analysis of He, Ne, H₂, O₂, N₂ by means of a molecular sieve 5A (20 meter unheated) column
243 and CO₂, CH₄ and H₂S by means of a PoraPlot (PPQ 10 meter heated) column. The instrument is
244 equipped with a micro thermal conductivity detector (TCD) responding to the difference in
245 thermal conductivity between the carrier gas (argon) and the sample composition. The detection
246 limit is 1 ppm, operating range is from 1 ppm to 100% level concentrations, and repeatability is
247 < 0.5% RSD in peak area at constant temperature and pressure.

248 For the analysis of $\delta^{13}\text{C}_{\text{CO}_2}$, carbon dioxide was cryogenically removed from the gas
249 samples by liquid nitrogen and measured by Thermo Finnigan Delta ^{PLUS} XP isotope ratio mass
250 spectrometer. Isotope ratios are given in the standard δ notation in permil (‰) versus VPDB.
251 Errors for $\delta^{13}\text{C}$ are 0.5‰.

252 Noble gas isotopic ratios ($^3\text{He}/^4\text{He}$ and $^4\text{He}/^{20}\text{Ne}$) were measured from each gas sample
253 that was inserted into the preparation line of the VG5400 noble gas mass spectrometer. The
254 argon and the other chemically active gases (N₂, CO₂ etc.) were separated in a cryogenic cold
255 system consisting of two cold traps and were adsorbed in an empty trap at 25K. The Ne and He
256 were adsorbed in a charcoal trap at 10K. He was desorbed at 42K and neon at 90K and measured

257 sequentially. The measurement procedure was calibrated with known air aliquots. The analytical
258 uncertainties are 1% for He concentrations and 5% for Ne concentrations and 2.5% for $^3\text{He}/^4\text{He}$.
259 $^3\text{He}/^4\text{He}$ ratio is expressed as R/Ra (being Ra the He isotope ratio of air and equal to $1.384 \cdot 10^{-6}$).
260 He isotopic composition was corrected for the atmospheric He contamination (R/R_{ac}) considering
261 the $^4\text{He}/^{20}\text{Ne}$ ratio; $R/R_{ac} = [R/R_a \cdot (X-1)] / (X-1)$ where X is the air-normalized $^4\text{He}/^{20}\text{Ne}$ ratio
262 taken as 0.318 (Sano & Wakita, 1985).

263 For the samples of the second analysis campaign, the chemical and isotopic composition
264 of He-Ne and $^{13}\text{C}_{\text{CO}_2}$ was determined in the laboratories of INGV-Palermo.

265 The concentrations of CO_2 , CH_4 , O_2 and N_2 were analysed using an Agilent 7890B gas
266 chromatograph with Ar as carrier and equipped with a 4-m Carbosieve S II and PoraPlot-U
267 columns. A TCD detector was used to measure the concentrations of He, O_2 , N_2 and CO_2 and a
268 FID detector for CO and CH_4 . The analytical errors were 10% for He and 5% for O_2 , N_2 , CO,
269 CH_4 and CO_2 . More details on the analytical procedures used during this analysis are given in
270 Liotta & Martelli (2012).

271 The carbon isotopic composition of CO_2 ($\delta^{13}\text{C}_{\text{CO}_2}$) was determined using a Thermo Delta
272 XP IRMS equipped with a Thermo Scientific™ TRACE™ Ultra Gas Chromatograph, and a 30
273 m Q-plot column (i.e. of 0.32 mm). The resulting $\delta^{13}\text{C}_{\text{CO}_2}$ values are expressed in ‰ with respect
274 to the international V-PDB (Vienna Pee Dee Belemnite) standard and analytical uncertainties are
275 $\pm 0.15\%$. The method for the $\delta^{13}\text{C}$ determination of Total Dissolved Carbon (TDC) is based on
276 chemical and physical CO_2 stripping (Capasso et al., 2005a). Isotopic ratios were measured using
277 a Finnigan Delta Plus Mass Spectrometer. The results are expressed in ‰ of the international V-
278 PDB standard. The standard deviations of the $^{13}\text{C}/^{12}\text{C}$ ratios are $\pm 0.2\%$.

279 ^3He , ^4He and ^{20}Ne and the $^4\text{He}/^{20}\text{Ne}$ ratios were determined by separately inserting He
280 and Ne into a split flight tube mass spectrometer (GVI-Helix SFT, for He analysis) and into a
281 multi-collector mass spectrometer (Thermo-Helix MC plus, for Ne analysis), after standard
282 purification procedures (Rizzo et al., 2015). The analytical reproducibility was $< 0.1\%$ for ^4He
283 and ^{20}Ne . However, the estimation of He and Ne concentration agrees within 10% uncertainty
284 respect to GC measurements. In this study, the time from sampling to analysis was lower than
285 two weeks and results are fully reliable. The analytical error for He and Ne concentration
286 measurements is generally below 0.3%.

287 3.2 Noble gas isotope data for the Perşani clinopyroxene

288 The chosen xenolith is a fresh spinel lherzolite with about 12% clinopyroxene content.
289 Here, we performed new noble gas analyses. The preparation, single-step crushing and analysis
290 of fluid inclusions was the same as described by Correale et al. (2012) and references therein.
291 Helium (^3He and ^4He) isotopes were measured separately by two different split-flight-tube mass
292 spectrometers (Helix SFT-Thermo). The analytical uncertainty of the determination of the TGC
293 and the He, Ne, abundances was $\sim 10\%$. Error in the $^3\text{He}/^4\text{He}$ ratios is reported at the 1σ level.
294
295
296

297 4. Results

298 The site, sample names and geographical locations with their GPS coordinates (WGS84,
299 Geographical Coordinates), source type (mofettes or bubbling pools), temperature, pH and
300 electrical conductivity for bubbling pool samples are presented in **Table 1**, chemical and isotopic
301

302 composition are listed in **Table 2 and 3**. Noble gas isotopic compositions of clinopyroxenes
303 from mantle xenoliths are shown in **Table 4**.

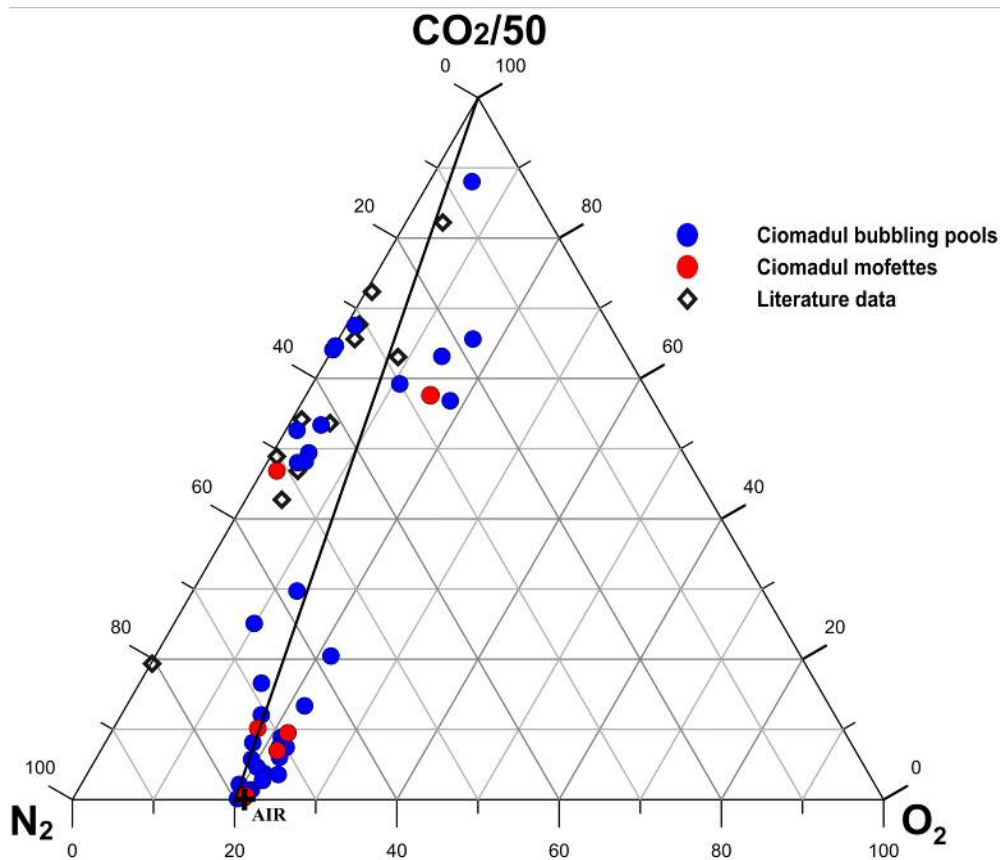
304

305 **4.1 Chemical and isotopic composition of gases**

306

307 The CO₂ concentration in the collected gases ranges from 6.40 to 98.36%. Besides CO₂, H₂S
308 (2.7×10^{-4} to 1.72×10^{-1} %), He (5.91×10^{-5} to 1.66×10^{-2} %), Ne (6.39×10^{-7} to 5.80×10^{-3} %), H₂
309 (1×10^{-5} to 2.3×10^{-1} %) CO (6×10^{-5} to 5×10^{-4} %), CH₄ (3.5×10^{-2} to 1.69%), N₂ (1.5×10^{-1} to 74.5%),
310 and O₂ (2×10^{-3} to 18.99) are present in the gas samples. The ternary diagram CO₂/50-N₂-O₂
311 (**Figure 3**) shows a progressive enrichment in N₂ and O₂ of the samples, indicating a variable
312 amount of air.

313



314

315

316 **Figure 3:**CO₂/50 - O₂ - N₂ triangular diagram showing the relative contents of components. The samples distribution
317 highlights mixing between CO₂ and atmospheric gas species. Literature data from Ciomadul area is represented by
318 data from [Althaus et al., 2000](#); [Vaselli et al., 2002](#); [Frunzeti, 2013](#)).

319

320 Table 2.

321 *Chemical composition of the different gas samples, expressed in %.*

322 Note. Nd= not determined

323

324

325 Table 3.

326 *Isotopic composition of the gas samples.*

327 *Note.* $^3\text{He}/^4\text{He}$ ratios are normalized to the atmosphere and listed as R/R_a values corrected for the atmospheric He
328 contamination (R/R_{ac}) considering the $^4\text{He}/^{20}\text{Ne}$ ratio; $\delta^{13}\text{C}\text{-CO}_2$ and $\delta^{18}\text{O}\text{-CO}_2$ are expressed in ‰ vs. VPDB.
329 Nd=not determined

330
331 The $^3\text{He}/^4\text{He}$ ratios range between 0.77 to 3.10 R_a and the $^4\text{He}/^{20}\text{Ne}$ ratios from 0.36 and 1700,
332 which show that some of the collected gases are affected by air contamination (**Table 3**). The
333 $^3\text{He}/^4\text{He}$ ratios after corrections for the air contamination (R/R_{ac}) are up to 3.25. The $\delta^{13}\text{C}_{\text{CO}_2}$
334 ranges between -1.40‰ and -17.2‰ vs. V-PDB (**Table 3**).

335

336 **4.2 Noble gas ratios of fluid inclusions from Persani clinopyroxenes**

337

338 Helium content in the fluid inclusions in clinopyroxenes ranged between 4.06×10^{-12} and
339 3.81×10^{-12} mol/g, Ne content between 2×10^{-15} and 2.74×10^{-15} mol/g, so the He/Ne ratios ranged
340 between 1390 and 2030. The He isotopic signature in fluid inclusions was $5.95 R_a \pm 0.01$ (**Table**
341 **4**).

342

343 Table 4.

344 *Isotopic composition of Persani clinopyroxene.*

Sample	He mol/g	Ne mol/g	He/Ar	$^4\text{He}/^{20}\text{Ne}$	R/Ra	R/Rac
Cpx xenolith	4.06E-12	2.00E-15	0.92	2030.46	5.96	5.96
Cpx xenolith 2	3.81E-12	2.74E-15	0.91	1389.41	5.94	5.94

345 *Note.* $^3\text{He}/^4\text{He}$ ratios are normalized to the atmosphere and listed as R/R_a values and corrected for the atmospheric
346 helium.

347

348 **5. Discussion**

349

350 **5.1 Crustal assimilation vs. mantle metasomatism**

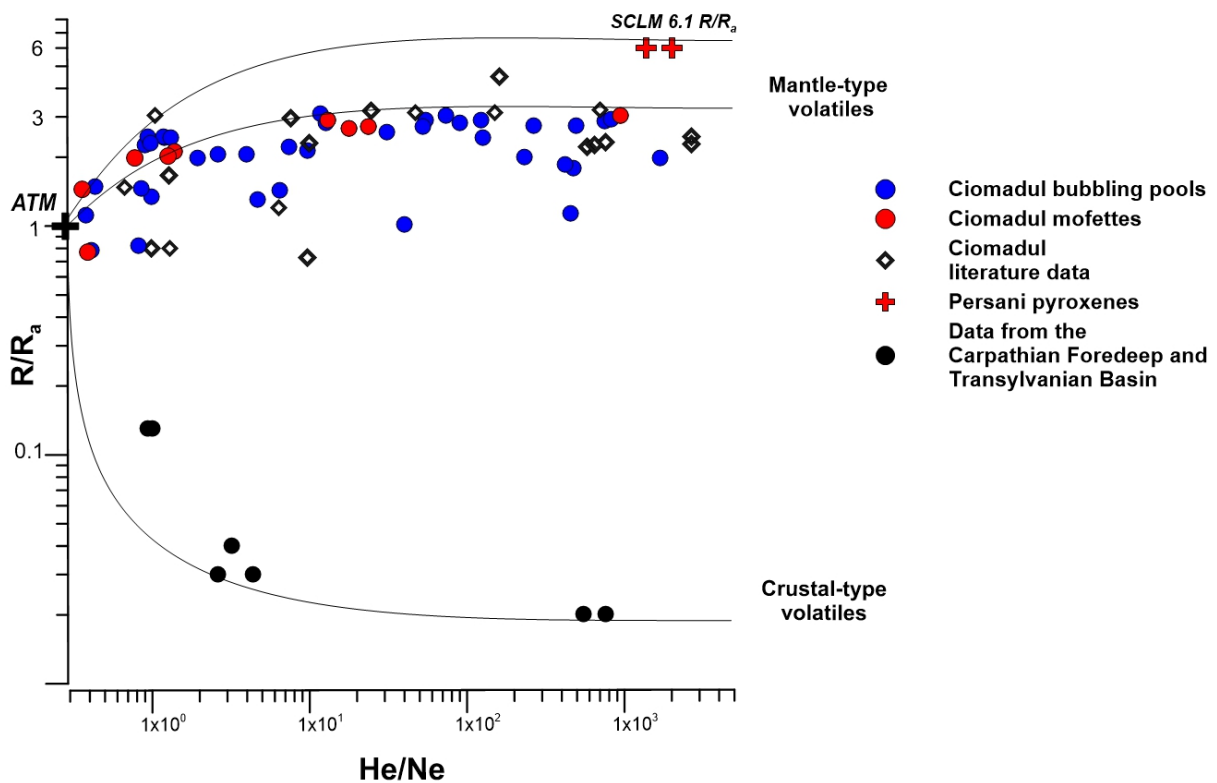
351

352 Helium comes from three different sources (mantle, crust and air), which can be readily
353 distinguished based on their characteristic isotopic ratios (Sano & Wakita, 1985). Helium
354 isotopes are useful tracers for detecting deep fluids and their possible origin (crust, mantle or
355 atmosphere) (Ozima and Podosek 2002). It has been demonstrated that in the case of quiescent
356 volcanoes, the active degassing of deep volatiles can occur for a long time after the last volcanic
357 activity (Carapezza et al., 2007; Tassi et al., 2013; Caracausi et al., 2009 and 2015).

358 The last eruption in Ciomadul occurred 30 ka (Harangi et al., 2010; 2015b; Molnár et al., 2019),
359 yet there is an intense CO_2 degassing with a minimum flux of $8.7 \times 10^3 \text{ t yr}^{-1}$ (Kis et al., 2017),
360 which is comparable to other dormant volcanic areas such as Panarea ($1.72 \times 10^4 \text{ t yr}^{-1}$) and
361 Roccamonfina ($7.48 \times 10^3 \text{ t yr}^{-1}$) from Italy or Jefferson ($7.92 \times 10^3 \text{ t yr}^{-1}$) from the USA.

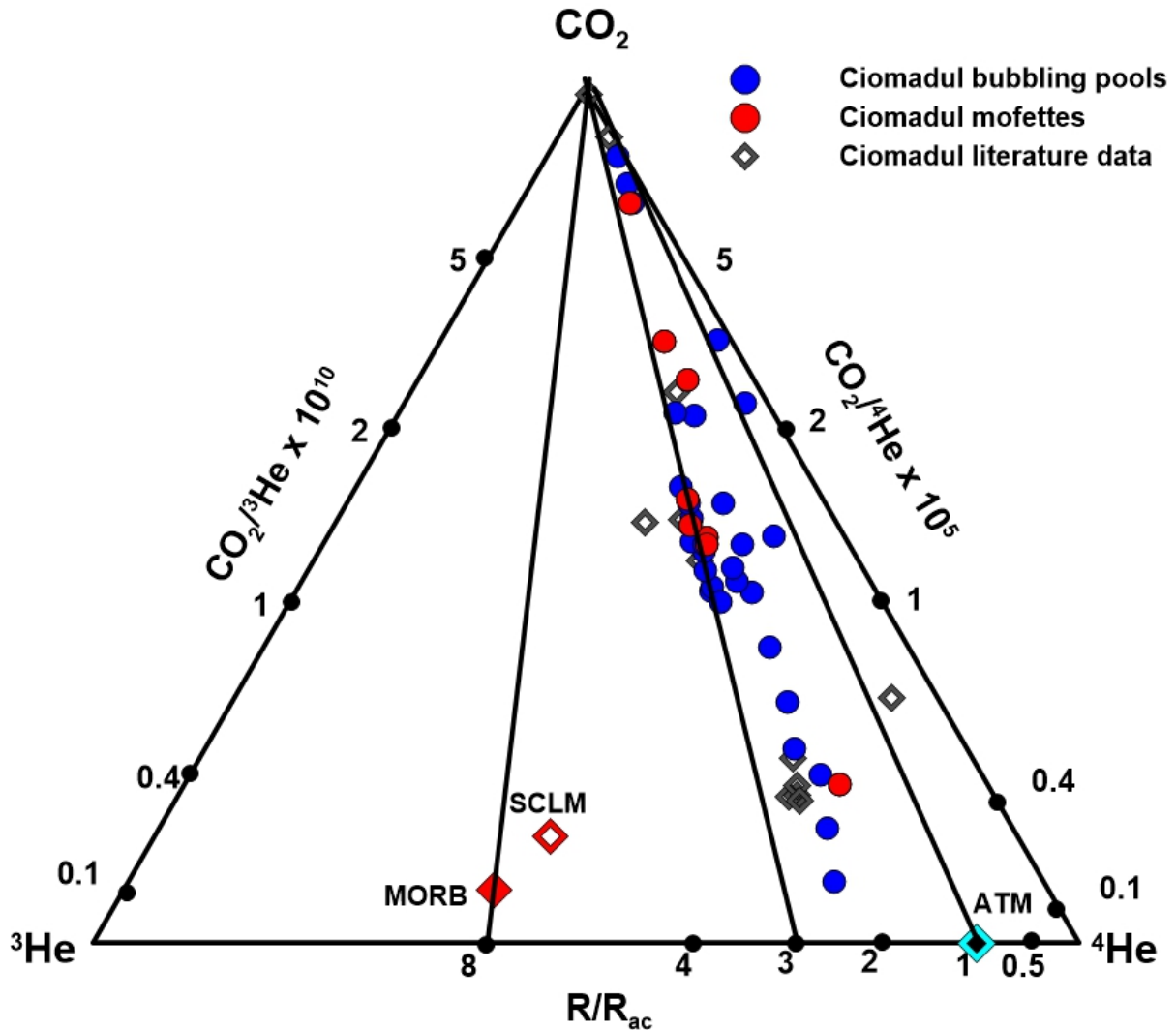
362 In addition, previous investigations (Althaus et al., 2000; Vaselli et al., 2002) highlighted the
363 outgassing of mantle-derived volatiles at Ciomadul volcano. He isotopic ratios in the fluids
364 collected in this study are up to $3.1 R_a$ similar to those obtained from previous studies (**Figure 4**,
365 **Table 3**). These values are higher than those obtained from the surrounding areas such as in the
366 Carpathian Foredeep and the Transylvanian Basin where He isotopic ratios are between 0.02 and

367 0.03R_a (Vaselli et al., 2002; Italiano et al., 2017; Baciu et al., 2017, **Figure 4**). These latter
 368 values are typical of crustal fluids dominated by ⁴He produced by decay of U and Th (e.g.,
 369 Ozima and Podosek, 2002). The higher R_a values measured at Ciomadul could imply a higher
 370 contribution of magmatic He. Nevertheless, the 3.1 R_a value is significantly lower than the
 371 MORB and SCLM value (Sano & Marty, 1995) requiring addition of radiogenic ⁴He that
 372 decreased the pristine isotopic signature.
 373 The mantle xenoliths of the Perșani volcanic field (ca. 40 km from the Ciomadul area) could
 374 provide the He isotopic signature of the lithospheric mantle beneath the region. The He isotopic
 375 ratios in fluid inclusions of the Persani clinopyroxenes are 5.95±0.01 (**Table 4**) and these are
 376 lower than those of previous measurements, from 6.5 to 7.3R_a, obtained by Althaus et al.
 377 (1998), but consistent with the values of the Subcontinental Lithospheric Mantle (SCLM, R/R_a =
 378 6.1 ± 0.9 R_a, Gautheron & Moreira, 2002). The continental crust (R/R_a=0.02, Ozima and
 379 Podosek, 2002) and atmosphere (R/R_a=1) have distinct isotopic values and ⁴He/²⁰Ne can be used
 380 to infer how mixing between the three possible end-members can support the He isotopic
 381 signature of the fluids that outgas in the Ciomadul region (**Figure 4**). Most Ciomadul samples
 382 indicate a possible trend between air and a magmatic source, where the He ratio of the magmatic
 383 end-member (3.1R_a) is lower than that of the ECLM and the Perșani clinopyroxene. This is also
 384 supported by the trend line in the ³He–CO₂–⁴He ternary diagram (**Figure 5**), where the Ciomadul
 385 samples are along a trend showing variable amounts of CO₂ and R/R_{ac} values between 2 and 3.
 386 This trend reflects the dominance of radiogenic He in the fluids outgassing from the Ciomadul
 387 volcano. We have now to assess the possible processes that can add the radiogenic He
 388 component to the mantle component.
 389



390
 391

392 **Figure 4:** Helium isotopic ratios (R/R_a values) and $^4\text{He}/^{20}\text{Ne}$ relationships. The theoretical lines represent binary
 393 mixings of atmospheric He with mantle-originated and crustal He (Pik & Marty, 2008). The assumed end members
 394 for He-isotopic ratios and $^4\text{He}/^{20}\text{Ne}$ ratios are: ATM ($1 R_a$, $\text{He}/\text{Ne}=0.318$, Sano and Wakita 1985); Subcontinental
 395 European Mantle ($6.1 \pm 0.9 R_a$ and $^4\text{He}/^{20}\text{Ne}$ ratio=1000; Gautheron and Moreira, 2002); typical crustal end-member
 396 is $0.02 R_a$ and $^4\text{He}/^{20}\text{Ne}$ ratio = 1000 (Sano and Marty, 1995). Literature data for comparison: data after Althaus et al.
 397 2000; Vaselli et al. 2002; Baciú et al., 2007; 2017; Frunzetti et al., 2013).
 398



399
 400
 401 **Figure 5:** Ternary CO_2 - ^3He - ^4He diagram of Ciomadul gas samples. Ciomadul literature data after Althaus et al.
 402 2000, Vaselli et al. 2002, Frunzetti et al., 2013. For reference, we have plotted the MORB (Marty & Jambon, 1987)
 403 and SCLM values (Gautheron and Moreira, 2002)
 404

405 Such a relatively low He isotope ratio of the magma source is not uncommon in volcanic arc
 406 settings (e.g., Hilton et al., 1992; Allard et al., 1997; Inguaggiato et al., 1998; Martelli et al.,
 407 2004) and can be due to several processes involving the addition of radiogenically-produced ^4He ,
 408 such as magma aging, crustal assimilation, mixing between mantle and crustal-derived fluids,
 409 among others (Torgersen et al., 1995; Kennedy et al., 2006). Unfortunately, there are no
 410 undifferentiated mantle-derived mafic rocks in the region of the Ciomadul volcano, so we cannot
 411 investigate the He isotope composition of the mantle directly below the volcano. In Ciomadul,

412 only high-K dacitic volcanic products are found (Mason et al., 1996; Vinkler et al., 2007; Molnár
413 et al., 2018; 2019), although occurrence of high-Mg minerals such as olivine and clinopyroxene
414 in the dacites suggest involvement of primitive mafic magmas in the magma evolution of
415 Ciomadul (Vinkler et al., 2007; Kiss et al., 2014).

416
417 Magma aging and crustal assimilation are two mechanisms that could account for the addition of
418 the radiogenic He component to the mantle-derived melts. Both these processes have been
419 invoked to explain low He isotopic ratios ($<$ MORB and SCLM) in different volcanic regions,
420 worldwide, such as Aeolian Island, Italy (Mandarano et al., 2015) and Iceland (Condomines et
421 al., 1993). The magma-aging mechanism considers an addition of ^4He by radiogenic decay in the
422 magma itself. In contrast, crustal assimilation furnishes ^4He by interaction between magma and
423 the whole rock. First, we investigated the likelihood that the magma aging model can interpret
424 the low He isotopic signature in the fluids that outgas at Ciomadul volcano.

425 The $^3\text{He}/^4\text{He}$ ratio of the fluid inclusions of the Persani clinopyroxene ($5.95R_a \pm 0.01$) can be
426 assumed to represent the mantle end-member value beneath of the region. Thus, the primary
427 magmas of Ciomadul could be also characterized by such isotope ratio. The Ciomadul dacites
428 have U and Th concentrations of 3 and 15 ppm respectively (Vinkler et al., 2007; Molnár et al.,
429 2018; 2019). Using these data, the magma-aging model calculation yield $^3\text{He}/^4\text{He}$ ratio around
430 $4.65R_a$ after 30 kyr (Figure 6). Thus, this process alone cannot be responsible for the low He (ca.
431 $3.1R_a$) isotopic signature of the Ciomadul fluids. Furthermore, if we assume the U (1.5ppm) and
432 Th (5.5 ppm) contents of the Persani basalts (Harangi et al., 2013), the magma-aging model is
433 still not a viable process to provide the required ^4He addition and generate the low $^3\text{He}/^4\text{He}$ for
434 Ciomadul gases.

435 The relatively low He isotopic ratio can also be explained by high-level crustal assimilation (e.g.,
436 van Soest et al., 2002), which has to also be evaluated. Assuming the U and Th amount of the
437 typical upper crust, 2.7 and 10.5 ppm, respectively (Rudnick and Gao, 2014) and an age of 5Ma,
438 3% of crustal assimilation could be sufficient to achieve the observed low He isotopic ratios. The
439 Sr-Nd-O isotope compositions of the erupted magmas sensitively reflect such a process. Mason
440 et al. (1996) published isotopic data for three samples of the Ciomadul volcanic system. They
441 have distinct isotopic features compared to the calc-alkaline volcanic suite of the Calimani-
442 Gurghiu-Harghita chain. Although the Sr-Nd isotopic data could suggest an AFC process with
443 10-35% assimilation of flysch sediment, such a high crustal contamination is not feasible, based
444 on the fairly low $\delta^{18}\text{O}$ values (6.3-7.1 per mil) of the phenocrysts from the dacites (Mason et al.,
445 1996). Instead, they suggested that these isotopic characteristics could also be explained by
446 source contamination from subduction-related fluids. In fact, the bulk-rock composition of the
447 Ciomadul dacites has unique characteristics with high Sr, Ba (both showing typically >1000
448 ppm) and high K compositions and low concentrations of heavy rare-earth elements (Seghedi et
449 al., 1987; Vinkler et al., 2007; Molnár et al., 2018; 2019). Furthermore, the high-Mg pargasitic
450 amphiboles thought to have derived from the less differentiated magmas have also relatively
451 high Ba content (Kiss et al., 2014). Thus, these peculiar compositional characters can be due to
452 the nature of the magma source rather than magma differentiation processes. The elevated K, Sr
453 and Ba contents of the assumed mantle source of the Ciomadul primary magmas can be due to
454 metasomatism and this is in contrast what the peridotite xenoliths from the Persani volcanic field
455 show (Vaselli et al., 1995). In fact, the He signature of the outgassed volatiles at Ciomadul
456 resembles the values in fluids from other subduction-related volcanic systems (i.e., Italy, Greece,
457 Indonesia; Hilton et al., 1992; Martelli et al., 2004; Shimizu et al., 2005), where the mantle

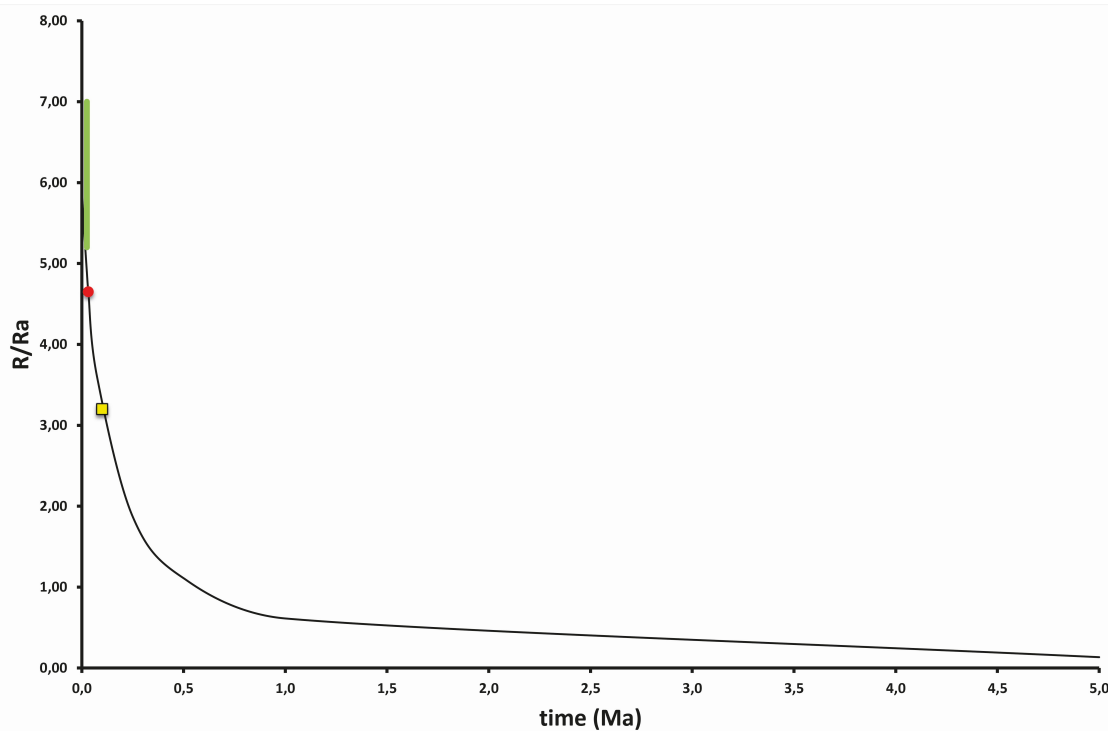
458 source regions seem to be contaminated by crustal material which added radiogenic ^4He and
459 decreased the pristine He isotopic signature (Hilton et al., 2002).
460 Such a small-scale spatial heterogeneity of the lithospheric mantle beneath this area can be
461 explained by the closer location of Ciomadul to the collision front, where subduction is expected
462 to have occurred during the Miocene up to around 11 Ma (Royden et al., 1982; Cloetingh et al.
463 2004; Matenco et al., 2007; Seghedi et al., 2011). Such a scenario is not unique, Martelli et al.
464 (2004) suggested that the relatively low He isotopic ratio in the volcanic rocks of Central Italy
465 can be explained by magma source features (i.e., contribution of radiogenic He from
466 metasomatic, subduction-related fluids and ingrowth of ^4He in the lithospheric mantle). We note
467 that the $^{87}\text{Sr}/^{86}\text{Sr}$ isotopic ratio of the Ciomadul dacites and the highest $^3\text{He}/^4\text{He}$ isotopic values
468 of the emitted gases plot into the same trend (Figure. 5 in Martelli et al., 2004) what the Central
469 Italian volcanic areas form.
470 In summary, considering the petrology of the Ciomadul volcanic products, the relatively low He
471 isotope magmatic end-member of the Ciomadul gases can be interpreted as due to magma-source
472 characteristics, where the radiogenic He was added via subduction-related fluids and increased
473 radioactive ingrowth following the metasomatism. However, a mixing between mantle-derived
474 fluids with and SCLM He isotopic signature and ^4He -rich crustal fluids coming from shallow
475 crustal layers should still be further explored as a possible process responsible of the low He
476 isotopic ratios in the Ciomadul fluids. This likelihood will be discussed in the next section.
477

478 5.2 Sources and origin of carbon-dioxide

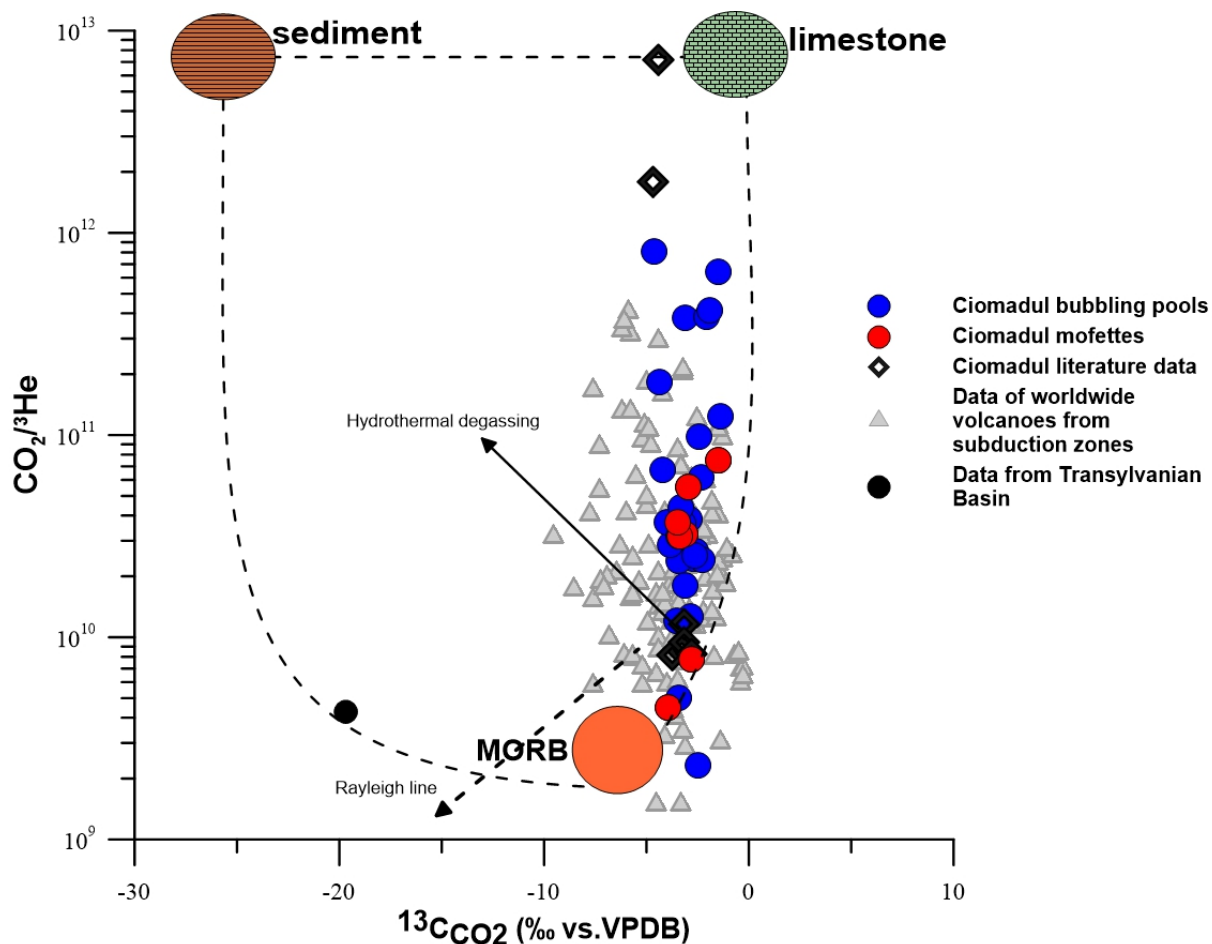
479
480 The carbon isotopic composition of CO_2 ($\delta^{13}\text{C}_{\text{CO}_2}$) from the studied fluids range between -
481 1.40‰ and -4.61‰ vs. VPDB, consistent with previous measurements in the area (-2.77 to -
482 4.70‰; Vaselli et al., 2002; Frunzeti, 2013; Sarbu et al., 2018). In the Pannonian Basin (central
483 Europe), the carbon isotopic composition of CO_2 gases shows values in a narrow range between -
484 3 to -7‰ with an average value of -5‰ V-PDB based on hundreds of measurements (Cornides,
485 1993; Sherwood-Lollar et al., 1997; Palcsu et al., 2014; Bräuer et al., 2016). These values are
486 consistent with a mantle origin. In contrast, crustal-derived CO_2 is characterized by a $\delta^{13}\text{C}$ of
487 about -25‰ in case of biogenic sedimentary source and around 0 ‰ considering thermo-
488 metamorphism of limestone (Sano&Marty, 1995 and references therein). The Ciomadul gases
489 overlap the range of mantle composition, even if some samples have more positive values that
490 cannot be explained by the addition of a crustal biogenic component (**table 3 and Figures 7 and**
491 **8**). To constrain the origin of CO_2 in the fluids emitted by the Ciomadul volcano, we used the
492 relationship between the elemental ratio $\text{CO}_2/{}^3\text{He}$ and the isotopic signature $\delta^{13}\text{C}_{\text{CO}_2}$ (Sano and
493 Marty, 1995; **Figure 7**).

494 The $\text{CO}_2/{}^3\text{He}$ ratios of the Ciomadul gases are higher than 2×10^9 , the expected mantle ratio
495 (Marty and Jambon, 1987) and which suggests an addition of a crustal component. It is
496 interesting that these ratios fall into the same trend as shown by volcanic and fumarolic gases
497 measured at volcanic arcs, worldwide (Mason et al., 2017; **Figure 8a and b**). Almost all the
498 Ciomadul samples fall close the mixing line between a mantle component and a limestone end-
499 member suggesting that mixing of the two sources could be the main process that controls the
500 CO_2 - ${}^3\text{He}$ systematics in these fluids. In contrast, CO_2 fluids in the Transylvanian Basin, (Baciu et
501 al., 2007, 2017) west of the volcano have distinct character and fall closer to the mantle – organic
502 sediment mixing line. Rayleigh-type fractionation due to gas exsolution from water is not a
503 plausible process to produce the carbon isotopic signature and the $\text{CO}_2/{}^3\text{He}$ of the studied fluids
504 (**Figure 7**) (Holland&Gilfilland, 2013; Roulleau et al., 2015). However, the $^{13}\text{C}_{\text{CO}_2}$ values of

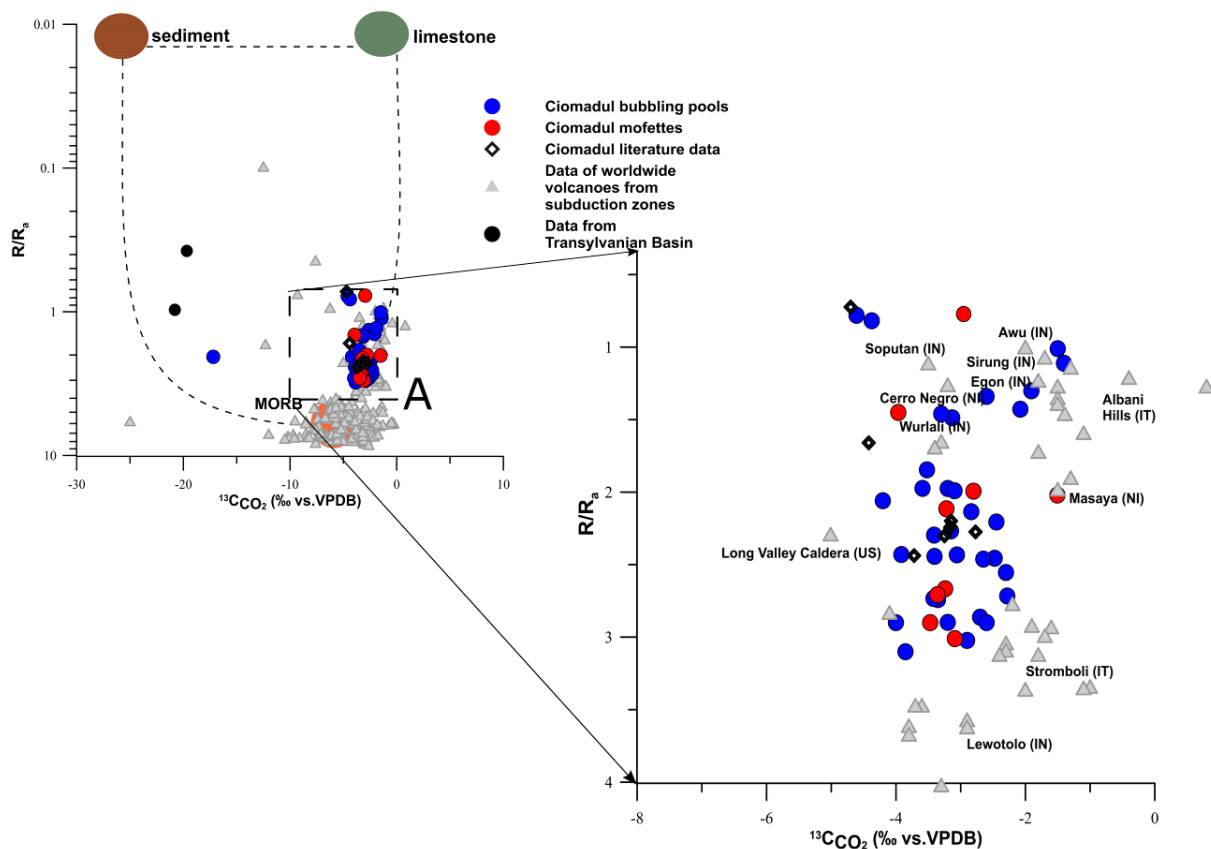
505 most of the samples fall in the narrow range of -2 and -5‰, which is a typical signature for
 506 mantle-derived carbon. We obtain the same trend in the He isotopic ratios (R/R_a) vs. $^{13}\text{C}_{\text{CO}_2}$ (V-
 507 PDB) plot (**Figure 8a and b**), where the Ciomadul samples clearly approach the mantle end-
 508 member and overlap the isotopic values of many other volcanic systems related to subduction
 509 areas. Remarkably the Ciomadul samples show similarities in He-C isotopic composition with
 510 active and dormant volcanic regions (e.g., Italy and Indonesia).
 511 The involvement of carbonatic component can be explained by mixing with fluids derived from
 512 thermometamorphic decomposition of carbonates in the flysch sedimentary pile or by mantle
 513 source contamination via subducted carbonatic material. The mantle source of the Ciomadul
 514 magmas is considered to be a metasomatic lithospheric mantle based on the compositional
 515 features of the dacitic rocks. The relatively low He isotopic ratio can be due to these source
 516 characteristics, whereas metasomatism was the result of slab-derived fluids during the Miocene
 517 subduction along the Eastern Carpathians followed by ingrowth of radiogenic He by radioactive
 518 decay. The Sr-Nd-O isotope data of the volcanic rocks do not support significant upper-level
 519 crustal contamination, but rather crustal component addition to the source region via slab-derived
 520 fluid metasomatism (Mason et al., 1996). The combination of He and C isotopic data suggests
 521 that this crustal component consisted of decomposed subducted carbonate material as suggested
 522 also for the volcanic rocks in Italy, although addition of fluids from carbonate decomposition at
 523 shallow crustal level cannot be unambiguously excluded.
 524



525
 526
 527 **Figure 6** Magma aging evolution over time of the He isotopic signature (as R/R_a). The green bar is the range of the
 528 SCLM He isotopic ratio (6.1 ± 0.9 ; Gautheron and Moreira, 2002). The red circle is the value of the $^3\text{He}/^4\text{He}$ ($4.65R_a$)
 529 at 30 ka for the magma aging evolution. $^3\text{He}/^4\text{He} = 3.2$ is at 100ka (yellow square).
 530
 531



532
 533 **Figure 7:** Correlation diagram of [Sano and Marty \(1995\)](#) plotting $\text{CO}_2/{}^3\text{He}$ vs. ${}^{13}\text{C}_{\text{CO}_2}$ (VPDB) of Ciomadul gas
 534 emissions. Lines show the theoretical mixing between a mantle end-member and a crustal end-member represented
 535 by marine limestone and organic sediment carbon. Ciomadul samples are showing a trend of mixing between fluids
 536 of mantle origin and fluids originating from limestone. Literature data for comparison: data after [Althaus et al. 2000](#);
 537 [Vaselli et al. 2002](#); [Baciu et al., 2007](#); 2017; [Frunzeti et al., 2013](#).
 538 Data on individual volcanoes worldwide based on the compilation of [Mason et al. \(2017\)](#), by [Allard, 1983](#); [Marty &](#)
 539 [Giggenbach, 1990](#); [Poorter et al., 1991](#); [Varekamp et a., 1992](#); [Sturchio et al., 1993](#); [Sano et al., 1994](#); [Sano &](#)
 540 [Marty, 1995](#); [Tedesco et al., 1995](#); [Hilton, 1996](#); [Sano&Williams, 1996](#); [Allard et al., 1997](#); [Fischer et al., 1998](#); [Van](#)
 541 [Soest et al., 1998](#); [Pedroni et al., 1999](#); [Lewicki et al., 2000](#); [Parello et al., 2000](#); [Favara et al., 2001](#); [Snyder et al.,](#)
 542 [2001](#); [Shaw et al., 2003](#); [Symonds et al., 2003](#); [Jaffe et al., 2004](#); [Capasso et al, 2005b](#); [Carapezza et al., 2007](#); [de](#)
 543 [Leeuw et a., 2007](#); [Werner et al., 2009](#); [Capaccioni et al., 2011](#); [Tassi et al., 2011](#); [Aguilera. et al., 2012](#); [Melian et](#)
 544 [al., 2012](#); [Caracausi et al., 2013](#).
 545
 546



547
 548 **Figure 8a and b** Correlation diagram (Ciotoli et al., 2013) plotting He isotopic ratios (R/R_a) vs. $^{13}\text{CO}_2$ (VPDB) of
 549 Ciomadul gas emissions. Lines show the theoretical mixing between a mantle end-member (MORB) and a crustal
 550 end-member represented by marine limestone and organic sediment carbon (Sano & Marty, 1995, Sherwood Lollar,
 551 Frunzeti et al., 2013). Literature data for comparison: data after Althaus et al. 2000; Vaselli et al. 2002; Baciu et al., 2007, 2017;
 552 Frunzeti et al., 2013. Data on individual volcanoes worldwide based on the compilation of Mason et al. (2017) from
 553 the data presented by Allard., 1983; Marty & Giggenbach, 1990; Poorter et al., 1991; Varekamp et al., 1992;
 554 Sturchio et al., 1993; Sano et al., 1994; Sano & Marty, 1995; Tedesco et al., 1995; Hilton, 1996; Sano & Williams,
 555 1996; Allard et al., 1997; Fischer et al., 1998; Van Soest et al., 1998; Pedroni et al., 1999; Lewicki et al., 2000;
 556 Parello et al., 2000; Favara et al., 2001; Snyder et al., 2001; Shaw et al., 2003; Symonds et al., 2003; Jaffe et al.,
 557 2004; Capasso et al., 2005b; Carapezza et al., 2007; de Leeuw et al., 2007; Werner et al., 2009; Capaccioni et al.,
 558 2011; Tassi et al., 2011; Aguilera et al., 2012; Melian et al., 2012; Caracausi et al., 2013.

560 5.3 Relationship with the deep magmatic system

561
 562 Dormant volcanoes pose a particular hazard to society since there is much less awareness
 563 about a possible eruption event. However, the scientific community is giving increased attention
 564 to these volcanoes and the surrounding areas that are generally characterized by intense gas
 565 emissions (Burton et al., 2013 and references therein). Recent investigations highlighted the
 566 presence of an active plumbing system even below volcanoes which last erupted >10 kyr (e.g.,
 567 Colli Albani, Italy; Trasatti et al., 2018; Uturuncu, Bolivia; Sparks et al., 2008; Comeau et al.,
 568 2015; Tatun, Taiwan; Konstantinou et al., 2007; Lin & Pu, 2016). Harangi et al. (2015a)
 569 suggested the term PAMS volcano, i.e. volcano with Potentially Active Magma Storage for these
 570 long-dormant volcanoes, which have clear implication for a subvolcanic melt-bearing magma
 571 plumbing system. Ciomadul belongs to this category, since there are a number of observations
 572 suggesting that a melt-bearing magma body could still exist beneath it (Popa et al., 2012;

573 Szakács and Seghedi, 2013; Harangi et al., 2015a). The isotopic composition of the emitted gases
574 coupled to the high localized heat flow in the area of the Ciomadul volcano gives additional
575 support to this interpretation.

576 This involves the similarities in the isotope composition of CO₂ and He of the gases emitted at
577 the Ciomadul with those found in other active and dormant volcanic arc systems worldwide and
578 their proposed high magmatic component. Furthermore, the Ciomadul volcanic system is
579 characterized by relatively high CO₂ gas fluxes (Kis et al., 2017). This is consistent with the
580 presence of a still-degassing magma below the Ciomadul system as inferred by geophysical
581 investigations that recognized a low-resistivity and low-velocity anomaly in the crust, below the
582 volcano (Popa et al., 2012; Harangi et al., 2015a) as well as petrologic observations suggesting
583 the involvement of a mafic magma in the petrogenesis of the erupted dacite (Kiss et al., 2014).
584 The measurements of U-Th and U-Pb spot ages on zircons suggest a long-standing magma
585 storage that could go back as far as about 350 ka (Harangi et al. 2015b; Lukács et al., 2018).
586 Molnár et al. (2018; 2019) presented a detailed eruption chronology for the Ciomadul lava dome
587 field involving the Ciomadul volcanic complex and emphasized that volcanic activity could be
588 renewed even after long (>100 kyr) repose times. Several 10's kyr quiescence periods between
589 the active phases have also been pointed out also during the evolution of the Ciomadul volcanic
590 complex (Harangi et al., 2015b; Molnár et al., 2019). However, the zircon U-Th and U-Pb ages
591 suggest that crystallization was on-going also during the long quiescence periods, i.e. there was
592 an active magma storage beneath the apparently inactive volcano. This suggests a long-standing
593 felsic upper-crustal crystal mush system underlain by a mafic hot zone in the lower crust, as has
594 already been suggested by petrologic interpretations (Kiss et al. 2014). The diverse amphibole
595 compositions in the dacites are consistent with a polybaric magma evolution, i.e. with
596 transcrustal magma storage (Cashman et al., 2017; Sparks & Cashman, 2017) comprising
597 ephemeral melt-dominated bodies, i.e. magma chambers at various depths. In addition, fluid-gas
598 accumulation zones can also have developed within this magma storage (Christopher et al.,
599 2015; Sparks & Cashman, 2017). Thus, a possible source of the CO₂ gases could be these fluid
600 entrapment zones within the crystal mush during quiescent period. However, gas emission is
601 more common around the Ciomadul volcanic complex and significantly lower within the volcano
602 itself (Kis et al. 2017). Allard et al. (1991) and Edmonds (2008) pointed out that stronger
603 degassing around the volcanic edifice is not uncommon in volcanic regions. An alternative
604 source of the CO₂ gases could be mafic magma residing at deeper level, possibly at the lower
605 crust. Indeed, the occurrence of high-Mg minerals, such as olivine, clinopyroxene and
606 orthopyroxene in the dacites (Vinkler et al., 2007; Kiss et al., 2014) suggests that mafic magma
607 also played an important role in the magma evolution. Harangi et al. (2015a) detected a lower
608 crustal low resistivity anomaly, which might represent the mafic magma accumulation. Thus, we
609 propose that most of the CO₂ gases could come directly from the presumed mafic-magma
610 accumulation zone at the lower crust through fractures (Kis et al., 2017), whereas only limited
611 amount of gases are derived from the mushy magma storage.

612 Vaselli et al. (2002) already suggested that the emitted gases in Southern Harghita could have
613 a magmatic component. Based on our new measurements, we support this interpretation,
614 particularly in the area of Ciomadul volcano. Assuming that a deep-seated mafic magma body
615 can be the main source of the CO₂ gases and considering that it is characterized by relatively low
616 ³He/⁴He isotope signature (3.1R_a) inherited by the mantle source region, we can use this value to
617 calculate the relative magmatic component of the emitted gases (Sano & Wakita, 1985). If no
618 interaction with crustal fluids occurred, the magmatic component in the gases could exceed even

619 the 80%. Remarkably, we obtained such high values for the areas having a larger diffusive CO₂
620 flux. This high magmatic He content of the gases is not unique and resembles what [Trasatti et al.](#)
621 [\(2018\)](#) proposed for Colli Albani volcanic complex, another long-dormant volcanic field, where
622 they assumed more than 80% mantle-derived component in the emitted CO₂ gases. However, the
623 magmatic component can be lower, if interaction between the ascending gases with crustal gases
624 occurred at shallow crustal depth, a possibility what we cannot test at this stage, but requires
625 further studies.

626

627 **Conclusions**

628

629 We investigated 31 gas emissions at the Ciomadul volcano, a long-dormant PAMS volcano
630 in eastern-central Europe, to constrain the origin of the emitted volatiles and the possible
631 processes that modify their chemistry during the transfer of these fluids towards the surface. The
632 carbon and helium isotopic compositions provide evidence for a significant magmatic
633 component. Our study shows a clear magmatic component in the emitted fluids and the highest
634 values correspond to the area characterized by the highest CO₂ flux from soil, so the high fluxes
635 can be associated with the highest contribution of volatiles derived from a magma body.
636 The relatively large CO₂ gas emission and significant magmatic component of the gases are
637 consistent with geophysical and petrologic models ([Popa et al., 2012](#); [Harangi et al., 2015a,](#)
638 [2015b](#)), that a degassing magmatic intrusion could still exist beneath Ciomadul. A long-standing
639 silicic crystal mush body should be developed in the shallow crust, while a mafic magma
640 accumulation zone is inferred at the lower crustal level. The magmatic gases could be derived
641 either from a deep mafic magma and/or from the volatile accumulation zones developed in the
642 shallow crustal felsic-crystal mush body. Petrology and geochemistry of the erupted dacitic
643 magma imply that upper crustal contamination played no or subordinate role and the primary
644 magmas could have derived from a mantle source contaminated by subduction-related fluids that
645 is consistent with the He and C isotope composition of the gases emitted at Ciomadul volcano.
646 Thus, a magma source with relatively low He isotope value (3.10 R_a), similar what was proposed
647 for volcanic systems in central Italy and Greece seems to be viable beneath Ciomadul. This
648 differs from the SCLM value detected at the nearby Persani volcanic field ([Althaus et al. 1998](#);
649 [this study](#)) and also in the Pannonian basin ([Cornides, 1993](#); [Palcsu et al., 2014](#); [Bräuer et al.,](#)
650 [2016](#)) and requires a spatially-variable modified lithospheric mantle even a small scale. The
651 isotopic composition (He and CO₂) of the emitted volatiles implies interaction of crustal gases to
652 varying degrees, although some of them could reach the surface without major modification.

653

654 **Acknowledgements**

655

656 Information regarding the support of the conclusions of this work can be found in the tables and
657 within the text.

658 This research on the Ciomadul volcano was initiated during the MTA Postdoctoral Fellowship of
659 Boglárka-Mercedesz Kis and belongs to the scientific project supported by the OTKA
660 (Hungarian National Research Fund) No. K116528. The research was also supported by the
661 European Union and the State of Hungary, co-financed by the European Regional Development
662 Fund in the project of GINOP-2.3.2-15-2016-00009 'ICER' and we acknowledge the support of
663 the Deep Energy Community of the Deep Carbon Observatory. Thorough reviews and
664 constructive comments provided by Emilie Roulleau and Daniele Pinti helped considerably to

665 clarify the ideas described in the paper. We thank Timothy Jull who provided a final polishing of
666 the English of the manuscript.

667

668 **References**

669

670 Aguilera, F., Tassi, F., Darrah, T., Moune, S. & Vaselli, O. (2012). Geochemical model of
671 magmatic-hydrothermal system at the Lastarria volcano, Northern Chile. *Bulletin of*
672 *Volcanology*, 74, 119–134. doi:10.1007/s00445-011-0489-5

673

674 Agosto M., Tassi F., Caselli A.T., Vaselli O., Rouwet D., Capaccioni B., Caliro S., Chiodini G.
675 & Darrah T. (2013). Gas geochemistry of the magmatic-hydrothermal fluid reservoir in the
676 Copahue-Cavahue Volcanic Complex (Argentina). *Journal of Volcanology and Geothermal*
677 *Research*, 257, 44–56. 10.1016/j.jvolgeores.2013.03.003

678

679 Allard, P. (1983). The origin of hydrogen, carbon, sulphur, nitrogen and rare gases in volcanic
680 exhalations: evidence from isotope geochemistry. In H. Tazieff, J.C. Sabroux, (Eds.) *Forecasting*
681 *Volcanic Events*, (pp.337–386), Amsterdam, Elsevier.

682

683 Allard, P., Carbonelle, J., Dajčević, D., Le Bronec, J., Morel, P., Robe, M.C., Maurenas, J.M.,
684 Faivre-Pierret, R., Martin, D., Sabroux, J.C., Zettwoon, P. (1991). Eruptive and diffuse emissions
685 of CO₂ from Mount Etna, *Nature*, 351, 387–391, doi:10.1038/351387a0

686

687 Allard, P., Jean-Baptiste, P., D'Alessandro, W., Parello, F., Parisi, B. & Flehoc, C. (1997).
688 Mantle-derived helium and carbon in groundwaters and gases of Mount Etna, Italy. *Earth and*
689 *Planetary Science Letters*, 148, 501–516

690

691 Althaus, A., Niedermann, S. & Erzinger, J. (1998). Noble gas in ultramafic mantle xenoliths in
692 the Persani Mountains, Transylvanian Basin, Romania. *Mineralogical Magazine*, 62A, 43–44

693

694 Althaus, T., Niedermann, S., Erzinger, J. 2000. Noble gas studies of fluids and gas exhalations in
695 the East Carpathians, Romania. *Chemie der Erde*. 60:189-207.

696

697 Aiuppa, A., Moretti, R., Federico, C., Giudice, G., Gurrieri, S., Liuzzo, M., Papale, P., Shinohara,
698 H. & Valenza, M. (2007). Forecasting Etna eruptions by real-time observation of volcanic gas
699 composition. *Geology*, 35(12), 1115–1118, doi:10.1130/G24149A.1

700

701 Baciu, C., Caracausi, A., Etiope, G., Italiano, F. (2007). Mud volcanoes and methane seeps in
702 Romania: main features and flux, *Annals of Geophysics*, 50, 4, doi: 10.4401/ag-4435

703

704 Baciu, C., Ionescu, A., Etiope, G., (2017). Hydrocarbon seeps in Romania: Gas origin and
705 release to the atmosphere, *Marine and Petroleum Geology*, 89, 1, 130–143, doi:
706 10.1016/j.marpetgeo.2017.06.015

707

708 Băncilă I. (1958). *Geology of the Eastern Carpathians*. Bucharest, Editura Stiintifica

709

710 Barry, P.H., Hilton, D.R., Fűri, E., Halldórsson, S.A. & Grönvold, K. (2014). Carbon isotope and
711 abundance systematics of Icelandic geothermal gases, fluids and subglacial basalts with
712 implications from mantle plume-related CO₂ fluxes. *Geochimica et Cosmochimica Acta*, 134, 74–
713 99. doi:10.1016/j.gca.2014.02.038
714
715 Barry, P.H., Hilton, D.R., Fischer, T.P., de Moor, J.M., Mangasini, F. & Ramirez, C. (2013).
716 Helium and carbon isotope systematic of cold “mazucu” CO₂ vents and hydrothermal gases and
717 fluid from Rungwe Volcanic Province, southern Tanzania. *Chemical Geology*, 339, 141–156. doi:
718 10.1016/j.chemgeo.2012.07.003
719
720 Berszán J., Jánosi Cs., Jánosi K., Kristály F., Péter É., Szakáll S. & Ütő G. (2009). *The mineral*
721 *waters of Szeklerland*. Miercurea Ciuc, Tipographic (In Hungarian)
722
723 Bräuer, K., Geissler, W.H., Kämpf, H., Niedermann, S., Rman, N. (2016). Helium and carbon
724 isotope signatures of gas exhalations in the westernmost part of the Pannonian Basin (SE
725 Austria/NE Slovenia): Evidence for active lithospheric mantle degassing. *Chemical Geology*, 422,
726 60–70, doi: 10.1016/j.chemgeo.2015.12.016
727
728 Bräuer, K., Kämpf, H., Niedermann, S., Strauch, G. & Tesar J. (2008). Natural laboratory NW
729 Bohemia: Comprehensive fluid studies between 1992 and 2005 used to trace geodynamic
730 processes. *Geochemistry, Geophysics, Geosystems*, 9(4), 1–30. doi: 10.1029/2007GC001921
731
732 Bräuer, K., Kämpf, H., Niedermann, S. & Strauch, G. (2018). Monitoring of helium and carbon
733 isotopes in the western Eger Rift area (Czech Republic): Relationships with the 2014 seismic
734 activity and indications for recent (2000–2016) magmatic unrest. *Chemical Geology*, 482, 131–
735 145. 10.1016/j.chemgeo.2018.02.017
736
737 Caliro, S., Viveiros F., Chiadini, G. & Ferreira, T. (2015). Gas geochemistry of hydrothermal
738 fluids of the S. Miguel and Terceira Islands, Azores. *Geochimica et Cosmochimica Acta*, 168,
739 43–57. doi: 10.1016/j.gca.2015.07.009
740
741 Capaccioni, B., Aguilera, F., Tassi, F., Darrah, T., Poreda, R. & Vaselli, O. (2011). Geochemical
742 and isotopic evidences of magmatic inputs in the hydrothermal reservoirs feeding the fumarolic
743 discharges on Tacora volcano (Northern Chile). *Journal of Volcanology and Geothermal*
744 *Research*, 208, 77–85. doi:10.1016/j.jvolgeores. 2011.09.015
745
746 Capasso, G., Carapezza, M., Federico, C., Inguaggiato, S. & Rizzo, A. (2005b). Geochemical
747 monitoring of the helium isotopic composition of fumarole gases and thermal waters. *Bulletin of*
748 *Volcanology*, 68, 118–134. doi:10.1007/s00445-005-0427-5
749
750 Capasso, G., Favara, R., Grassa, F., Inguaggiato, S. & Longo, M. (2005a). On-line technique for
751 preparation and measuring stable carbon isotope of total dissolved inorganic carbon in water
752 samples ($\delta^{13}\text{C}_{\text{TDIC}}$). *Annals of Geophysics*, 48(1), 159–166. doi:10.1.1.1002.372
753

754 Caracausi A., Nuccio P.M., Favara R., Nicolosi M. & Paternoster M. (2009). Gas hazard assessment at
755 the Monticchio crater lakes of Mt. Vulture, a volcano in southern Italy. *Terra Nova*, 21, 83–
756 87, doi:10.1111/1365-3121.200800858
757

758 Caracausi, A., Favara, R., Giammanco, S., Italiano, F., Paonita, A., Pecoraino, G. & Rizzo A. (2003). Mount
759 Etna: Geochemical signals of magma ascent and unusually extensive plumbing system. *Geophysical
760 Research Letters*, 30(2), 1057, doi:10.1029/2002GL015463
761

762 Caracausi A., Martelli, M., Nuccio, P.M., Paternoster, M. & Stuart, F.M. (2013). Active degassing
763 of mantle-derived fluid: A geochemical study along the Vulture line, southern Apennines
764 (Italy). *Journal of Volcanology and Geothermal Research*, 253, 65–74,
765 10.1016/j.jvolgeores.2012.12.005
766

767 Caracausi, A., Paternoster M. & Nuccio P.M. (2015). Mantle CO₂ degassing at Mt. Vulture volcano (Italy):
768 Relationship between CO₂ outgassing of volcanoes and the time of their last eruption. *Earth and Planetary
769 Science Letters*, 411, 268–280, doi:10.1016/j.epsl.2014.11.049
770

771 Carapezza, M. L., Badalamenti, B., Cavarra, L. & Scalzo, A. (2003). Gas hazard assessment in a
772 densely inhabited area of Colli Albani Volcano (Cava dei Selci, Roma). *Journal of Volcanology
773 and Geothermal Research*, 123, 81–94, doi: 10.1016/S0377-0273(03)00029-5
774

775 Carapezza, M.L., Barbieri, F., Ranaldi, M., Ricci, T., Tarchini, L., Barrancos, J., Fischer, C.,
776 Granieri, D., Lucchetti, C., Melian, G., Perez, N., Tuccimei, P., Vogel, A. & Weber, K.
777 (2012). Hazardous gas emissions from the flanks of the quiescent Colli Albani volcano (Rome,
778 Italy). *Applied Geochemistry*, 27, 1767–1782, doi: 10.1016/j.apgeochem.2012.02.012
779

780 Carapezza, M.L. & Tarchini, L. (2007). Accidental gas emission from shallow pressurized
781 aquifers at Alban Hills volcano (Rome, Italy): Geochemical evidence of magmatic degassing?
782 *Journal of Volcanology and Geothermal Research*, 165, 5–16.
783 doi:10.1016/j.jvolgeores.2007.04.008
784

785 Cardellini, C., Chiodini, G., Frondini, F., Avino, R., Bagnato, E., Caliro, S., Lelli, S. & Rosiello,
786 A. (2017). Monitoring diffuse volcanic degassing during volcanic unrest: the case of Campi
787 Flegrei (Italy). *Scientific Reports*, 7, 6757, doi:10.1038/s41598-017-06941-2
788

789 Cashman, K.V., Sparks, S., Blundy, J.D. (2017). Vertically extensive and unstable magmatic
790 systems: An unified view of igneous processes. *Science*, 355, 6331, doi: 10.1126/eaay3055
791

792 Ciotoli, G., Etiope, G., Florindo, F., Marra, F., Ruggiero, L. & Sauer, P.E. (2013). Sudden deep
793 gas eruption nearby Rome's airport of Fiumicino. *Geophysical Research Letters*, 40, 1–5,
794 doi:10.1002/2013GL058132
795

796 Christopher, T.E., Blundy, J., Cashman, K., Cole, P., Edmonds, M., Smith, P.J., Sparks, R.S.J.,
797 Stinton, A. (2015). Crustal-scale degassing due to magma system destabilization and magma-gas
798 decoupling at Soufriere Hills Volcano, Montserrat, Geochemistry, Geophysics, Geosystems, 16,
799 9, 2797–2811, doi: 10.1002/2015GC005791
800

801 Christopher, T., Edmonds, M., Humphreys, M.C.S. & Herd, R.A. (2010). Volcanic gas emissions
802 from Soufriere Hills Volcano, Montserrat 1995-2009, with implications for mafic magma supply
803 and degassing. *Geophysical Research Letters*, 37, L00E04, doi: 10.1029/2009GL041325
804

805 Comeau, M.J., Unsworth, M.J., Ticona, F. & Sunagua, M. (2015). Magnetotelluric images of
806 magma distribution beneath Volcano Uturuncu, Bolivia: Implications for magma
807 dynamics. *Geology*, 43(3), doi:10.1130/G36258.1
808

809 Comeau, J.M., Unsworth, M.J. & Cordell, D. (2016). New constraints on the magma distribution
810 and composition beneath Volcan Uturuncu and the southern Bolivian Altiplano from
811 magnetotelluric data, *Geosphere*, 12(5), 1391–1421, doi: 10.1130/GES01277.1
812

813 Condomines, M., Gronvold K., Hooker P.J., Muehlenbachs, O’Nions R.K., Oskarsson N.
814 & Oxburgh E.R., (1983). Helium, oxygen, strontium and neodymium isotopic relationships in
815 Iceland volcanics. *Earth Planet. Sci. Lett.*, 66, 125-136.
816

817 Cornides I. (1993). Magmatic carbon dioxide at the crust’s surface in the Carpathian Basin,
818 *Geochemical Journal*, 27, 241–249, 10.2343/geochemj.27.241
819

820 Correale, A., Martelli, M., Paonita, A., Rizzo, A., Brusca, L. & Scribano, V. (2012). New evidence
821 of mantle heterogeneity beneath the Hyblean Plateau (southeast Sicily, Italy) as inferred from
822 noble gases and geochemistry of ultramafic xenoliths. *Lithos*, 132–133, 70–81,
823 10.1016/j.lithos.2011.11.007
824

825 Csontos, L., Nagymarosy, A., Horváth, D. & Kovác, M. (1992). Tertiary evolution of the intra
826 Carpathian area: a model. *Tectonophysics*, 208, 221–241
827

828 Cloetingh, S.A.P.L., Burov, E., Matenco, L., Toussaint, G., Bertotti, G., Andriessen, P.A.M.,
829 Wortel, M.J.R. & Spakman, W. (2004). Thermo-mechanical controls on the mode of continental
830 collision in the SE Carpathians (Romania). *Earth and Planetary Science Letters*. 218 (1–2): 57–
831 76. doi: 10.1016/S0012-821X(03)00645-9
832

833 de Leeuw, G., Hilton, D., Fischer, T.P. & Walker, J. (2007). The He-CO₂ isotope and relative
834 abundance characteristics of geothermal fluids in El Salvador and Honduras: new constraints on
835 volatile mass balance of the Central American Volcanic Arc. *Earth and Planetary Science
836 Letters*, 258, 132–146, doi: 10.1016/j.epsl.2007.03.028
837

838 Demetrescu, C. & Andreescu, M. (1994). On the thermal regime of some tectonic units in a
839 continental collision environment in Romania. *Tectonophysics*, 230(3-4), 265–276,
840 10.1016/0040-1951(94)90140-6
841

842 Downes, H., Seghedi, I., Szakács, A., Dobosi, G., James, D.E., Vaselli, O., Rigby, I.J.,
843 Ingram, G.A., Rex, D. & Pécskay, Z. (1995). Petrology and geochemistry of late
844 Tertiary/Quaternary mafic alkaline volcanism in Romania. *Lithos* 35(1-2), 65–81, 10.1016/0024-
845 4937(95)91152-Y
846

847 Edmonds, M.(2008). New geochemical insights into volcanic degassing, *Phil. Trans.R.Soc.A*,
848 366, 4559–4579, doi:10.1098/stra.2008.0185

849

850 Falus Gy., Tommasi, A., Ingrin, J. & Szabó Cs. (2008). Deformation and seismic anisotropy of
851 the lithospheric mantle in the southeastern Carpathians inferred from the study of mantle
852 xenoliths. *Earth and Planetary Science Letters*, 272, 50–64, doi:10.1016/j.epsl.2008.04.035

853

854 Farrar, C.D., Sorey, M.L., Evans, W.C., Howle, J.F., Kerr, B.D., Kennedy, B.M.,
855 King, C.Y. & Southon, J.R. (1995). Forest Killing diffuse CO₂ emission at Mammoth Mountain as a
856 sign of magmatic unrest. *Nature*, 376, 675–677, doi: 10.1038/376675a0

857

858 Favara, R., Giammanco, S., Inguaggiato, S. & Pecoraino, G. (2001). Preliminary estimate of
859 CO₂ output from Pantelleria Island volcano (Sicily, Italy): evidence for active mantle degassing.
860 *Applied Geochemistry*, 16, 883–894,

861

862 Fischer, T., Horalek, J, Hrubcova, P., Vavrycuk, V., Bräuer, K. & Kämpf, H. (2014). Intra-
863 continental earthquake swarms in West-Bohemia and Vogtland: A review. *Tectonophysics*, 611,
864 1–27, doi: 10.1016/j.tecto.2013.11.001

865

866 Fischer, T.P., Giggenbach, W.F., Sano, Y. & Williams, S.N. (1998). Fluxes and sources of
867 volatiles discharged from Kudryavy, a subduction zone volcano, Kurile Islands. *Earth and*
868 *Planetary Science Letters*, 160, 81–96, doi: 10.1016/S0012-821X(98)00086-7

869

870 Fischer, T.P. 2008. Fluxes of volatiles (H₂O, CO₂, N₂, Cl, F) from arc volcanoes. *Geochemical*
871 *Journal*, 42 (1), 21–38, 10.2343/geochemj.42.21

872

873 Frunzeti, N. (2013). *Geogenic emissions of greenhouse gases in the Southern part of the Eastern*
874 *Carpathians*, (Doctoral dissertation), Retrieved from Faculty of Environmental Science and
875 Engineering. Cluj-Napoca. Babes-Bolyai University (In Romanian)

876

877 Gautheron, C. & Moreira, M. (2002). Helium signature of the subcontinental lithospheric mantle,
878 *Earth and Planetary Science Letters*, 199, 39–47, 10.1016/S0012-821X(02)00563-0

879 Grasu, C., Catana, C. & Bobos, I. (1996). *Petrology of the flysch formations in the inner*
880 *Carpathians*. Bucharest, Editura Tehnica

881

882 Harangi Sz., Molnár M., Vinkler A.P., Kiss B., Jull A.J.T. & Leonard A.E. (2010). Radiocarbon
883 dating of the last volcanic eruptions of Ciomadul volcano, Southeast Carpathians, eastern-central
884 Europe. *Radiocarbon*, 52(3), 1498–1507, 10.1017/S0033822200046580

885

886 Harangi, S., Sági, T., Seghedi, I. & Ntaflos, T. (2013). Origin of basaltic magmas of Perșani
887 volcanic field, Romania: a combined whole rock and mineral scale investigation. *Lithos* 180–
888 181, 43–57. doi:10.1016/j.lithos.2013.08.025

889

890 Harangi Sz., Novák A., Kiss B., Seghedi I., Lukács R., Szarka L., Wesztergom V., Metwaly M. &
891 Gribovszki K. (2015a). Combined magnetotelluric and petrologic constrains for the nature of the

892 magma storage system beneath the Late Pleistocene Ciomadul volcano (SE Carpathians). *Journal*
893 *of Volcanology and Geothermal Research*, 290, 82–96, 10.1016/j.jvolgeores.2014.12.006
894

895 Harangi, Sz., Lukács, R., Schmitt, A.K., Dunkl, I., Molnár, K., Kiss, B., Seghedi, I., Novothny,
896 A., Molnár M. (2015b). Constraints on the timing of Quaternary volcanism and duration of
897 magma residence at Ciomadul volcano, east-central Europe, from combined U-Th/He and U-Th
898 zircon geochronology. *Journal of Volcanology and Geothermal Research*, 301, 66–80,
899 doi: 10.1016/j.jvolgeores.2015.05.002
900

901 Hilton, D.R., Hoogewerff, J.A., Van Bergen, M.J. & Hammerschmidt, K. (1992). Mapping
902 magma sources in the east Sunda-Banda arcs, Indonesia: constraints from helium isotopes,
903 *Geochimica et Cosmochimica Acta*, 56, 851-859
904

905 Hilton, D. (1996). The helium and carbon isotope systematics of a continental geothermal
906 system: results from monitoring studies at Long Valley caldera (California, U.S.A.). *Chemical*
907 *Geology*, 127, 269-295. doi: 10.1016/0009-2541(95)00134-4
908

909 Hilton, D.R., Fischer, T.P., Marty, B.(2002). Noble gases and volatile recycling at subduction
910 zones. *Rev. in Mineralogy and Geochemistry*, 47, 1, 319–370, doi:10.2138/rmg.2002.47.9
911

912 Holland G. & Gilfillan S., (2013). Application of the noble gases to the variability of CO₂
913 storage. In: *The noble gases as geochemical tracers*, Pete Burnad Editor, 177-223, Springer
914

915 Horváth, F., Bada, G., Windhoffer, G., Csontos, L., Dombradi, E., Dövényi, P., Fodor, L.,
916 Grenerczy, Gy., Síkhegyi, F., Szafián, P., Székely, B., Timár G., Tóth T., (2006). The
917 geodynamic atlas of the Pannonian Basin: Euro-conform maps and explanations, *Magyar*
918 *Geofizika*, 47, 4, 133–137 (In Hungarian).
919

920 Ianovici, V. and Rădulescu, D. (1968). Geological map 1:200000 L-35-XIV, 20th Sheet-Odorhei.
921 Geological Institute of Romania, Bucharest (In Romanian)
922

923 Ismail-Zadeh, A., Matenco, L., Radulian M., Cloetingh, S.& Panza, S. (2012). Geodynamics and
924 intermediate-depth seismicity in Vrancea (the south-eastern Carpathians): Current state-of-the
925 art. *Tectonophysics*, 530, 50–79, doi: 10.1016/j.tecto.2012.01.016
926

927 Italiano, F., Kis, B.M., Baciu, C., Ionescu, A., Harangi, Sz. & Palcsu, L. (2017). Geochemistry of
928 dissolved gases from the Eastern Carpathians-Transylvanian Basin boundary. *Chemical Geology*,
929 469, 117–128, 10.1016/j.chemgeo.2016.12.019
930

931 Jaffe, L.A., Hilton, D.R., Fischer, T.P.& Hartono, U. (2004). Tracing magma sources in an arc-
932 arc collision zone: Helium and carbon isotope and relative abundance systematics of the Sanhihe
933 Arc, Indonesia. *Geochemistry, Geophysics, Geosystems*, 5(4), Q04J10, doi:
934 10.1029/2003GC000660
935

936 János, Cs. (1980). *The hydrogeology of the inferior part of the Ciuc Basin, with focus on the*
937 *mineral water springs*. (Doctoral dissertation). Retrieved from Faculty of Biology and Geology.
938 Cluj-Napoca. Babes-Bolyai University. (In Romanian)
939

940 János Cs., Berszán J. & Péter É. (2011). *The mineral baths of Ciomadul Mountains*, Acta Siculica
941 2011, Miercurea Ciuc, (pp.41-56) In Hungarian.
942

943 Karátson, D. & Timár, G. (2005). Comparative volumetric calculations of two segments of the
944 Carpathian Neogene/Quaternary volcanic chain using SRTM elevation data: implications for
945 erosion and magma output rates. *Zeitschrift für Geomorphologie*, 140, 19–35, Supplementary
946 Issues
947

948 Karátson, D., Wulf, S., Veres, D., Magyar, E., Gertisser, R., Timár-Gabor A. et al. (2016). The
949 latest explosive eruptions of Ciomadul (Csomád) volcano, East Carpathians-A tephrostratigraphic
950 approach for the 51-29 ka BP time interval, *Journal of Volcanology and Geothermal Research*,
951 319, 29–51, 10.1016/j.jvolgeores.2016.03.005
952

953 Kato, A., Terakawa, T., Yamanaka, Y., Maeda, Y., Horikawa, S., Matsushiro, K. et al. (2015).
954 Preparatory and precursory processes leading up to the 2014 phreatic eruption of Mount Ontake.
955 Japan. *Earth, Planets and Space*, 67, 111, doi: 10.1186/s40623-015-0288-x
956

957 Kennedy, B.M., van Soest, M.C., (2006). A helium isotope perspective on the Dixie Valley,
958 Nevada, hydrothermal system. *Geothermics*, 35(1), 26–43, doi:
959 10.1016/j.geothermics.2005.09.004.
960

961 Kiss, B., Harangi, Sz, Ntaflos, T., Mason, P. & Pál-Molnár, E. (2014). Amphibole perspective to
962 unravel pre-eruptive processes and conditions in volcanic plumbing systems beneath
963 intermediate arc volcanoes: a case study from Ciomadul volcano (SE Carpathians).
964 *Contributions to Mineralogy and Petrology*, 167(986). doi:10.1007/s00410-014-0986-6.
965

966 Kis B.M., Ionescu, A., Cardellini, C., Harangi, Sz., Baciu, C., Caracausi, C. & Viveiros, F.
967 (2017). Quantification of carbon dioxide emissions of Ciomadul, the youngest volcano of the
968 Carpathian-Pannonian Region (Eastern-Central Europe, Romania). *Journal of Volcanology and*
969 *Geothermal Research*, 341, 119–130, doi: 10.1016/j.jvolgeores.2017.05.025
970

971 Konstantinou, K.I., Lin, C-H. & Liang, W-T. (2007). Seismicity characteristics of a potentially
972 active Quaternary volcano: The Tatun Volcano Group, northern Taiwan, *Journal of Volcanology*
973 *and Geothermal Research*, 160, 300–318, doi: 10.1016/j.volgeores.2006.09.009.
974

975 Lee, H., Muirhead, J., Fischer, T.P., Ebinger, C.J., Kattenhorn, S.A., Sharp, Z.D. et al. (2016).
976 Massive and prolonged deep carbon emissions associated with continental rifting. *Nature*
977 *Geoscience*, 9, 145–149. doi: 10.1038/ngeo2622.
978

979 Lewicki, J.L. Fischer, T., Williams S.N. (2000). Chemical and isotopic compositions of fluid at
980 Cumbal Volcani, Colombia: Evidence for magmatic contribution. *Bulletin of Volcanology*, 62,
981 347-361, doi:10.1007/s004450000100

982
983 Liotta, M. & Martelli, M. (2012). Dissolved gases in brackish thermal waters: an improved
984 analytical method. *Geofluids*, 12, 236–244, doi: 10.1111/j.1468-8123.2012.00365.x.
985
986 Lin, C.H. & Pu, H.C. (2016). Very-long-period seismic signals at the Tatun Volcano Group,
987 northern Taiwan. *Journal of Volcanology and Geothermal Research*, 328, 230–236, doi:
988 10.1016/j.volgeores.2016.11.007
989
990 Lukács, R., Guillong, M., Schmitt A.K., Molnár K., Bachman O., Harangi Sz. (2018). La-ICP-
991 MS and SIMS U-Pb and U-Th zircon geochronological data of Late Pleistocene lava domes of
992 the Ciomadul Volcanic Dome Complex (Eastern Carpathians). *Data in Brief*. 18, 808–813, doi:
993 10.16/j.dib.2018.03.100
994
995 Mandarano, M., Paonita, A., Martelli, M., Viccaro, M., Nicotra, E. & Millar I.L., (2016).
996 Revealing magma degassing below closed-conduit active volcanoes: Geochemical features of
997 volcanic rocks versus fumarolic fluids at Vulcano (Aeolian Islands, Italy). *Lithos*, 248–251, 272–
998 287, doi: 10.1016/j.lithos.2016.01.026.
999
1000 Martelli, M., Nuccio, P.M., Stuart, F.M., Burgess, R., Ellam, R.M. & Italiano F.
1001 (2004). Helium–strontium isotope constraints on mantle evolution beneath the Roman
1002 Comagmatic Province, Italy. *Earth and Planetary Science Letters*. 224, 295 – 308
1003
1004 Marty B. & Giggenbach, W.F. (1990). Major and rare gases at White Island volcano, New
1005 Zealand: origin and flux of volatiles. *Geophysical Research Letters*, 17, 247–250,
1006 doi:10.1029/GL017i003p00247
1007
1008 Marty B. & Jambon, A. (1987). C/3He in volatile fluxes from the solid Earth: Implications for
1009 carbon geodynamics. *Earth and Planetary Science Letters*, 83, 16–26, doi: 10.1016/0012-
1010 821X(87)90047-1
1011
1012 Mason, E., Edmonds, M., Turchyn, A. (2017). Remobilization of crustal carbon may dominate
1013 volcanic arc emissions, *Science*, 357, 290–294, doi: 10.1126/science.aan5049
1014
1015 Mason, P., Downes, H., Thirlwall, M.F., Seghedi, I., Szakács, A., Lowry, D., Matthey, D., (1996).
1016 Crustal assimilation as a major petrogenetic process in the East Carpathian Neogene and
1017 Quaternary Continental Margin Arc, Romania
1018
1019 Mațenco L. & Bertotti G. (2000). Tertiary tectonic evolution of the external East Carpathians
1020 (Romania). *Tectonophysics*, 316(3–4), 255–286, 10.1016/S0040-1951(99)00261-9
1021
1022 Mațenco L., Bertotti G., Leever K., Cloething S., Schmidt SM, Tărășoancă M. & Dinu C. (2007).
1023 Large-scale deformation in a locked collisional boundary: interplay between subsidence and
1024 uplift, intraphase stress, and inherited lithospheric structure in the large stage of the SE Carpathian
1025 evolution. *Tectonics*, 26(4), 1–29, doi: 10.1029/2006TC001951
1026

1027 Mazot, A., Rouwet, D., Taran, Y., Inguaggiato, S. & Varley, N. (2011). CO₂ and He degassing at
1028 El Chicón volcano, Chiapas, Mexico: gas flux, origin and relationship with local and regional
1029 tectonics. *Bulletin of Volcanology*, 73, 423–441, doi 10.1007/s00445-010-0443-y
1030
1031 Melián G., Tassi, F., Pérez, N., Hernández, P., Sortino, F., Vaselli, O. et al. (2012). A magmatic
1032 source for fumaroles and diffuse degassing from the summit crater of Teide Volcano (Tenerife,
1033 Canary Islands): a geochemical evidence for the 2004-2005 seismic-volcanic crisis. *Bulletin of*
1034 *Volcanology*, 74, 1465–1483, doi:10.1007/s00445-012-0613-1.
1035
1036 Molnár, K., Harangi, Sz., Lukács R., Dunkl I., Schmitt, A.K., Kiss B., Garamhegyi T. & Seghedi
1037 I. (2018). The onset of the volcanism in the Ciomadul Volcanic Dome Complex (Eastern
1038 Carpathians): eruption chronology and magma type variation. *Journal of Volcanology and*
1039 *Geothermal Research*, 354, 39–56, doi10.1016/j.jvolgeores.2018.01.025
1040
1041 Molnár, K., Lukács, R., Dunkl, I., Schmitt, A.K., Kiss, B., Seghedi, I., Szepesi, J. and Harangi, S. (2019). Episodes
1042 of dormancy and eruption of the Late Pleistocene Ciomadul volcanic complex (Eastern Carpathians, Romania)
1043 constrained by zircon geochronology., 373: 133-147. (2019)
1044
1045 Moriya, I., Okuno, M., Nakamura, T., Ono, K. & Seghedi, I. (1996). Radiocarbon ages of
1046 charcoal fragments from the pumice flow deposits of the last eruption of Ciomadul Volcano,
1047 Romania. *Summaries of Researches Using AMS at Nagoya University*, 3, 252–255.
1048
1049 Moriya, I., Okuno, M., Nakamura, E., Szakács, A. & Seghedi, I. (1995). Last eruption and its ¹⁴C
1050 age of Ciomadul Volcano, Romania. *Summaries of Researches Using AMS at Nagoya*
1051 *University*, 6, 82–91.
1052
1053 Moussallam, Y., Bani, P., Schipper, C.I., Cardona, C., Franco, L., Barnie, T., Amigo, A., Curtis,
1054 A., Peters, N., Aiuppa, A., Giudice, G. & Oppenheimer, C. (2018). Unrest and the Nevados de
1055 Chillan volcanic complex: a failed or yet to unfold magmatic eruption. *Volcanica*, 1(1), 19-32,
1056 10.30909/vol.01.01.1932
1057
1058 Nicolaescu, V. (1973). Contributions to the knowledge on the Cretaceous flysch of the western
1059 part of Bodoc Mts. *Studii și cercetări Geologie Geofizica, Geografie*, 18(2), 479-488, (In
1060 Romanian)
1061
1062
1063 O'Nions, R.K. & Oxburgh, E.R. (1988). Helium, volatile fluxes and the development of the
1064 continental crust. *Earth and Planetary Science Letters*, 90(3), 331-347. doi: 10.1016/0012-
1065 821X(88)90134-3
1066
1067 Oppenheimer, C., Fischer, T. P. & Scaillet, B. (2014). Volcanic degassing: process and impact.
1068 In H.D. Holland, & K.K. Turekian (Eds.), *Treatise on Geochemistry*, 2nd Edition, Oxford, (pp.
1069 111–179), Elsevier, doi: 10.1016/B978-0-08-095975-7.00304-1
1070
1071 Ozima, M. & Podosek, F.A. (2004). *Noble gas geochemistry*. Cambridge, Cambridge University
1072 Press
1073

1074 Palcsu, L., Vető, I., Futó, I., Vodila, G., Papp, L., Major, Z. (2014). In-reservoir mixing of
1075 mantle-derived CO₂ and metasedimentary CH₄-N₂ fluids. Noble gas and stable isotope study of
1076 two multistaged fields (Pannonian Basin System, W-Hungary). *Marine and Petroleum Geology*,
1077 54, 216–227, doi: 10.1016/j.marpetgeo.2014.03.013
1078

1079 Panaiotu, C.G., Jicha, B.R., Singer, B.S., Tugui, A., Seghedi, I., Panaiotu, A.G. & Necula, C.
1080 (2013). ⁴⁰Ar/³⁹Ar chronology and paleomagnetism of Quaternary basaltic lavas from the Perșani
1081 Mountains (East Carpathians). *Physics of the Earth and Planetary Interiors*, 221, 1–
1082 24.10.1016/j.pepi.2013.06.007
1083

1084 Panaiotu, C.G., Pécskay, Z., Hambach, U., Seghedi, I., Panaiotu, C.E., Tetsumaru, I., Orleanu,
1085 M. & Szakács, A. (2004). Short-lived Quaternary volcanism in the Persani Mountains (Romania)
1086 revealed by combined K–Ar and paleomagnetic data. *Geologica Carpathica*, 55(4), 333–339.
1087

1088 Paonita, A., Caracausi, A., Iacono-Marziano, G., Martelli, M. & Rizzo, A. (2012). Geochemical
1089 evidence for mixing between fluids exsolved at different depths in the magmatic system of
1090 Mt. Etna (Italy). *Geochimica et Cosmochimica Acta*, 84, 380–394. doi:10.1016/j.gca.2012.01.028
1091

1092 Paonita, A., Longo, M., Bellomo, S., D’Alessandro, W. & Brusca, L. (2016). Dissolved inert
1093 gases (He, Ne and N₂) as markers of groundwater flow and degassing areas at Mt. Etna volcano
1094 (Italy). *Chemical Geology*, 443, 10–20, doi: 10.1016/j.chemgeo.2016.09.018
1095

1096 Parello, F., Allard P., D’Alessandro W., C. Federico, C., Jean-Baptiste P. & Catani, O. (2000).
1097 Isotope geochemistry of Pantelleria volcanic fluids, Sicily Channel rift: a mantle volatile end-
1098 member for volcanism in southern Europe, *Earth and Planetary Science Letters*, 180 (3–4), 325-
1099 339, 10.1016/S0012-821X(00)00183-7
1100

1101 Pécskay, Z., Lexa, J., Szakács, A., Seghedi, I., Balogh, K., Konecny, V., Zelenka, T., Kovacs,
1102 M., Póka, T., Fülöp, A., Márton, E., Panaiotu, C. & Cvetkovic, V. (2006). Geochronology of
1103 Neogene magmatism in the Carpathian arc and intra-Carpathian area. *Geologica Carpathica*, 57
1104 (6), 511–530.
1105

1106 Pedroni, A., Hammerschidt, K. & Friedrichsen, H. (1999). He, Ne, Ar and C isotope systematics
1107 of geothermal emanations in the Lesser Antilles Islands Arc. *Geochimica et Cosmochimica Acta*,
1108 63, 515–532, doi:10.1016/S0016-7037(99)00018-6
1109

1110 Pik, R. & Marty, B. (2008). Helium isotopic signature of modern and fossil fluids associated with
1111 the Corinth rift fault zone (Greece): Implication for fault connectivity in the lower crust.
1112 *Chemical Geology*, 266 (1), 67–75, 10.1016/j.chemgeo.2008.09.024
1113

1114 Pizzino, L., Galli, G., Mancini, C., Quattrocchi, F. & Scarlato, P. (2002). Natural gas hazard (CO₂
1115 and ²²²Rn) within a quiescent volcanic region and its relations with tectonics: the case of
1116 Ciampino-Marino Area, Albani Hills Volcano, Italy. *Natural Hazards*, 27, 257–287,
1117 10.1023/A:1020398128649
1118

1119 Popa M., Radulian, M., Szakács A., Seghedi I. & Zaharia B. (2012). New seismic and
1120 tomography data in the southern part of the Harghita Mountains (Romania, Southeastern
1121 Carpathians): connection with recent volcanic activity. *Pure Applied Geophysics*, 169, 1557–
1122 1573, doi: 10.1007/s00024-011-0428-6
1123

1124 Poorter, R., Varekamp, J., Poreda, R., Van Bergen, M. & Kreuen, R. (1991). Chemical and
1125 isotopic compositions of volcanic gases from the east Sunda and Banda arcs,
1126 Indonesia. *Geochimica et Cosmochimica Acta*, 55(12), 3798–3807, doi:10.1016/0016-
1127 7073(91)90075-G
1128

1129 Rădulescu, D., Peter, E., Stanciu, C., Stefanescu, M., & Veliciu, S. (1981). Discussion on the
1130 geothermal anomalies within South Harghita Mountains. *Studii si Cercetari Geologie.,*
1131 *Geografie, Geofizica, Seria Geologie*, 26(2), 169–184, In Romanian.
1132

1133 Rizzo, A. L., Barbieri, F., Carapezza, M.L., Di Piazza, A., Francalanci, L., Sortino, F. &
1134 D’Alessandro, W. (2015). New mafic magma refilling a quiescent volcano: Evidence from He-
1135 Ne-Ar isotopes during the 2011–2012 unrest at Santorini, Greece. *Geochemistry, Geophysics,*
1136 *Geosystems*, 16, 798–814, 10.1002/2014GC005653
1137

1138 Royden, L.H., Horváth, F., Burchfiel, B.C. (1982). Transform faulting, extension and subduction
1139 in the Carpathian Pannonian Region, *GSA Bulletin*, 93, 8, 717–725, doi: 10.1130/0016-
1140 7606(1982)93
1141

1142 Roulleau, E., Sano, Y., Takahata, N., Yang, F.T., Takahashi, H.A. (2015). He, Ar, N and C
1143 isotope compositions in Tatun Volcanic Group (TVG), Taiwan: evidence for an important
1144 contribution of pelagic carbonates in the magmatic source. *Journal of Volcanology and*
1145 *Geothermal Research*, 303, 7–15, doi:10.1016/j.volgeores.2015.07.017
1146

1147 Roulleau, E., Tardani, D., Sano, Y., Takahata, N., Vinet, N., Bravo, et al. (2016). New insight
1148 from noble gas and stable isotopes of geothermal/hydrothermal fluids at Cavihue-Copahue
1149 Volcanic Complex: Boiling steam separation and water-rock interaction at shallow depth, *Journal*
1150 *of Volcanology and Geothermal Research*, 328, 70–83, doi: 10.1016/j.jvolgeores.2016.10.007
1151

1152 Rouwet, D., Sandri, L., Marzocchi, W., Gottsmann, J., Selva, J., Tonini, R. et al.
1153 (2014). Recognizing and tracking volcanic hazards related to non-magmatic unrest: a
1154 review. *Journal of Applied Volcanology*, 3, 1–17, 10.1186/s13617-014-0017-3
1155

1156 Rouwet D., Hidalgo S., Joseph E.P., González-Ilama G. (2017). Fluid Geochemistry and
1157 Volcanic Unrest: Dissolving the Haze in Time and Space. In: *Advances in Volcanology*, Berlin,
1158 Heidelberg, Springer, doi:10.1007/11157_2017_12
1159

1160 Rudnick R.L. & Gao S., (2003). Composition of the continental crust. *Treatise in Geochemistry*,
1161 3:1-64, DOI: 10.1016/B0-08-043751-6/03016-4
1162

1163 Ruzié, L., Moreira, M.& Crispi, O. (2012). Noble gas isotopes in hydrothermal volcanic fluids of
1164 La Soufrière volcano, Guadeloupe, Lesser Antilles arc. *Chemical Geology*, 304–305, 158–165,
1165 doi:10.1016/j.chemgeo.2012.02.012

1166 Sano, Y., Hirabayashi, J.-I., Oba, T.& Gamo, T.(1994).Carbon and helium isotopic ratios at
1167 Kusatsu-Shirane volcano, Japan, *Applied Geochemistry*, 9, 371–377 doi: 10.1016/0883-
1168 29274)90059-0

1169

1170 Sano Y., Kagoshima T., Takahata N., Nishio Y., Roulleau, E., Pinti, D.L.& Fischer, T.P.
1171 (2015).Ten-year helium anomaly prior to the 2014 Mt. Ontake eruption. *Scientific Reports*, 5,
1172 13069, doi:10.1038/srep13069

1173

1174 Sano Y.& Marty B.(1995). Origin of carbon in fumarolic gas from island arcs, *Chemical*
1175 *Geology*, 119, 265–214,doi: 10.1016/0009-2541(94)00097-R

1176

1177 Sano Y.& Wakita H.(1985). Geographical distribution of $^3\text{He}/^4\text{He}$ ratios in Japan: Implications
1178 for arc tectonics and incipient magmatism, *Journal of Geophysical Research*, 90, 8729–8741,
1179 10.1029/JB090iB10p08729F

1180

1181 Sano, Y.& Williams S.N. (1996). Fluxes of mantle and subducted carbon along convergent plate
1182 boundaries. *Geophysical Research Letters*, 23, 2749–2752, doi: 10.1029/96GL02260

1183

1184 Sarbu, S., Aerts J.W., Flot, J.F., Van Spanning, R.J.M., Baciú C., Ionescu, A., Kis, B.M. et al.
1185 (2018). Sulfur Cave (Romania), an extreme environment with microbial mats in a $\text{CO}_2\text{-H}_2\text{S/O}$
1186 gas chemocline dominated by mycobacteria. *International Journal of Speleology*, 42(2), 173–182,
1187 doi: 10.5038/1827-806X.47.2.2164

1188

1189 Seghedi, I., Maţenco, L., Downes, H., Mason, P.R.D., Szakács, A.& Pécskay, Z. (2011).
1190 Tectonic significance of changes in post-subduction Pliocene-Quaternary magmatism in the
1191 south east part of the Carpathian-Pannonian Region. *Tectonophysics*, 502, 146–157,
1192 10.1016/j.tecto.2009.12.003

1193

1194 Seghedi, I.& Szakács, A.(1994). The Upper Pliocene–Pleistocene effusive and explosive
1195 basalticvolcanism from the Perşani Mountains. *Romanian Journal of Petrology*, 76, 101–107

1196

1197 Seghedi, I., Popa, R.G., Panaiotu, C.G., Szakács, A.& Pécskay, Z. (2016). Short-lived eruptive
1198 episodes during the construction of a Na-alkalic basaltic field (Perşani Mountains, SE
1199 Transylvania, Romania, *Bulletin of Volcanology*, 78, 69 doi:10.1007/s00445-016-1063-y

1200

1201 Seghedi, I., Downes, H., Szakács, A., Mason, P.R.D., Thirlwall, M.F., Rosu, E., Pécskay, Z.,
1202 Marton, E.& Panaiotu, C. (2004). Neogene-Quaternary magmatism and geodynamics in the
1203 Carpathian-Pannonian region: a synthesis. *Lithos*, 72, 117–146.

1204

1205 Seghedi, I., Downes, H., Harangi, Sz., Mason, P.R.D. & Pécskay, Z. (2005) Geochemical
1206 response of magmas to Neogene–Quaternary continental collision in the Carpathian–Pannonian
1207 region: A review. *Tectonophysics*, 410, 485 – 499, doi:10.1016/j.tecto.2004.09.015

1208

1209 Seghedi, I., Szakács, A., Udrescu, C., Stoian, M., Graban, G. (1987). Trace element
1210 geochemistry of the South Harghita volcanic (East Carpathians). Calc-alkaline and shoshonitic
1211 associations. *Dari de Seama a Sedintelor Institutului Geologic si Geofizic*, 72, 73, 1
1212

1213 Shaw, A.M., Hilton, D.R., Fischer, T.P., Walker, J.A. & Alvarado, G.E. (2003). Contrasting He-
1214 C relationships in Nicaragua and Costa Rica: Insights into C cycling through subduction
1215 zones. *Earth and Planetary Science Letters*, 214, 499–513, doi: 10.1016/S0012-821X(03)00401-
1216 1
1217

1218 Sherwood-Lollar, B., Ballentine, C.J., Onions, R.K. (1997). The fate of mantle-derived carbon in
1219 a continental sedimentary basin: intergration of C He relationships and isotope signatures.
1220 *Geochimica et Cosmochimica Acta*, 61, 11, 2295–2307, doi: 10.1016/S0016-7037(97) 00083-5
1221

1222 Shimizu, A., Sumino, H., Nagao, K., Notsu, K., Mitropoulos, P. (2005). Variation in noble gas
1223 isotopic composition of gas samples from the Aegean arc, Greece. *Journal of Volcanology and
1224 Geothermal Research*, 140, 321-339.
1225

1226 Snyder, G., Poreda, R., Hunt, A. & Fehn, U. (2001). Regional variations in volatile composition:
1227 isotopic evidence for carbonate recycling in the Central American volcanic arc. *Geochemistry,
1228 Geophysics, Geosystems*, 2, 1057, doi: 10.1029/2001GC000163
1229

1230 Symonds, R.B., Poreda, R.J., Evans, W.C., Janik, C.J. & Ritchie, B.E. (2003). Mantle and crustal
1231 sources of carbon, nitrogen and noble gases in Cascade-Range and Aleutian-Arc volcanic
1232 gases. *US Geological Survey Open-File Report*, 03–436
1233

1234 Sorey, M.L., Evans, W.C., Kennedy, B.M., Farrar, C.D., Hainsworth, L.J. & Hausback, B. (1998).
1235 Carbon dioxide and helium emission from a reservoir of magmatic gas beneath Mammoth
1236 Mountain, California. *Journal of Geophysical Research, Solid Earth*, 103(7), 15303–15323
1237

1238 Sparks, S., Cashman, K. (2017). Dynamic magma systems: implications for forecasting volcanic
1239 activity. *Elements*, 13, 1, 35-40, doi:10.2113/gselements.13.1.35
1240

1241 Sparks, R.S.J., Folkes, C.B., Humphreys, M.C.S., Barfod, D.N., Clavero, J., Sunagua, M.C.,
1242 McNutt, S.R., & Pritchard, M.E. (2008). Uturuncu volcano, Bolivia: Volcanic unrest due to mid-
1243 crustal magma intrusion. *American Journal of Science*, 308, 727–769, doi:10.2475/06.2008.01.
1244

1245 Sturchio, N.C., Williams, S.N. & Sano, Y. (1993). The hydrothermal system of Volcan Purace,
1246 Colombia. *Bulletin of Volcanology*, 55, 289–296, doi:10.1007/BF00624356
1247

1248 Szakács A. & Seghedi I. (1987). Base surge deposits in the Ciomadul Massif (South Harghita
1249 Mountains), *Dari de Seama ale sedintelor Institutului Geologic Geofizic*, 74(1), 175-180
1250

1251 Szakács A. & Seghedi I. (1995). The Călimani-Gurghiu-Harghita volcanic chain, East
1252 Carpathians, Romania: volcanological features. *Acta Volcanologica*, 7, 145–153
1253

1254 Szakács, A., Seghedi, I. (2013). The relevance of volcanic hazard in Romania: is there any?
1255 Environmental Engineering and Management Journal. 12, 125–135. doi: 0,30638/eemj.2013.015
1256

1257 Szakács A., Seghedi I. & Pécskay Z.(1993). Peculiarities of South Harghita Mts. as terminal
1258 segment of the Carpathian Neogene to Quaternary volcanic chain, *Rev. Roum de Géol.*, 37, 21–
1259 36
1260

1261 Szakács A., Seghedi I., Pécskay Z. & Mirea V. (2015). Eruptive history of a low-frequency and
1262 low-output rate Pleistocene volcano, Ciomadul, South Harghita Mts., Romania, *Bulletin of*
1263 *Volcanology*, 77(12), doi: 10.1007/s00445-014-0894-7
1264

1265 Tassi, F., Aguilera, F., Benavente, O., Paonita, A., Chiodini, G., Caliro, S., Agosto, M., Gutierrez,
1266 F., Capaccioni, B., Vaselli, O., Caselli, A.& Saltori, O. (2016).Geochemistry of fluid discharges
1267 from Peteroa volcano (Argentina-Chile) in 2010-2015: insights into compositional changes
1268 related to the fluid source region(s), *Chemical Geology*, 432, 41–53,
1269 doi:10.1016/j.chemgeo.2016.04.007
1270

1271 Tassi F., Aguilera F., Darrah T., Vaselli O., Capaccioni B., Poreda R.J.& Delgado Huertas
1272 A.(2010).Fluid geochemistry of hydrothermal systems in the Arica-Parinacota, Taracapa and
1273 Antofagasta regions (northern Chile).*Journal of Volcanology and Geothermal Research*, 192, 1–
1274 15, doi: 10.1016/j.jvolgeores.2010.02.006
1275

1276 Tassi, F., Aguilera, F., Vaselli, O. Darrah, T.& Medina, E. (2011). Gas discharges from four
1277 remote volcanoes in Chile (Putana, Olca, Irruputuncu and Alitar): a geochemical survey. *Annals*
1278 *of Geophysics*, 54, doi: 10.4401/ag-5173
1279

1280 Tassi F., Nisi, B., Cardellini C., Capecchiacci F., Donnini M., Vaselli O., Avino R.& Chiodini G.
1281 (2013). Diffuse soil emission of hydrothermal gases (CO₂, CH₄, C₆H₆) at Solfatara crater (Campi
1282 Flegrei, Southern Italy), *Applied Geochemistry*, 35, 142–153, 10.1016/j.apgeochem.2013.03.020
1283

1284 Torgersen, T., Drenkard, S., Stute, M., Schlosser, P., Shapiro, A. (1995). Mantle Helium in-
1285 Ground Waters of Eastern North-America - Time and Space Constraints On Sources. *Geology*,
1286 23(8), 675–678, doi: 10.1130/0091-7613(1995)023<0675:MHIGWO>2.3.CO;2
1287

1288 Trasatti, E., Marra, F., Polcari, M., Etioppe, G., Ciotoli, G., Darrah, T. H., Tedesco, D., S.
1289 Stramondo, S., Florindo, F., & Ventura, G. (2018). Coeval uplift and subsidence reveal magma
1290 recharging near Rome (Italy). *Geochemistry, Geophysics, Geosystems*, 19, 1484–1498.
1291 doi:10.1029/2017GC007303
1292

1293 Tedesco, D., Miele, G., Sano Y.& Tardani, J.P. (1995).Helium isotopic ratio in Vulcano island
1294 fumaroles: temporal variations in shallow level mixing and deep magmatic supply.*Journal of*
1295 *Volcanology and Geothermal Research*, 64(1-2), 117–118 doi: 10.1016/0377-0273(94)00045-I
1296

1297 Túri, M., Palcsu, L. Papp, L., Horváth, A., Futó, I., Molnár, M., Rinyu, L., Janovics, R., Braun,
1298 M., Hubay, K., Kis, B.M., Koltai, G. (2016). Isotope characterization of the water and sediment

1299 in volcanic lake Saint Ana, East-Carpathians, Romania. *Carpathian Journal of Earth and*
1300 *Environmental Sciences*, 11, 2, 475-484
1301
1302 Van Soest, M., Hilton, D. & Kreulen, R. (1998). Tracing crustal and slab contributions to arc
1303 magmatism in the Lesser Antilles island arc using helium and carbon relationships in geothermal
1304 fluids. *Geochimica et Cosmochimica Acta*, 62, 3323–3335, doi: 10.1016/S0016-7037(98)00241-5
1305
1306 Vaselli, O., Downes, H., Thirlwall, M.F., Dobosi, G., Coradossi, N., Seghedi, I., Szakács, A. &
1307 Vannucci, R. (1995). Ultramafic xenoliths in Plio-Pleistocene alkali basalts from the Eastern
1308 Transylvanian Basin: depleted mantle enriched by vein metasomatism. *Journal of Petrology*,
1309 36(1), 23–53, 10.1093/petrology/36.1.23
1310
1311 Vaselli, O., Minissale, A., Tassi, F., Magro, G., Seghedi, I., Ioane, D. & Szakács, A.
1312 (2002). Ageochemical traverse across the Eastern Carpathians (Romania): constraints on the
1313 origin and evolution of the mineral waters and gas discharge. *Chemical Geology*, 182(2-4), 637–
1314 654, 10.1016/S0009-2541(01)00348-5
1315
1316 Vinkler A.P., Harangi Sz., Ntaflor T, Szakács A. (2007). Petrology and geochemistry of pumices
1317 from the Ciomadul volcano (Eastern Carpathians)-implications for petrogenetic processes,
1318 *Földtani Közlemény* 137(1), 103–128, In Hungarian
1319
1320 Wei, F., Xu, J., Shangguan Z., Pan, S., Yu, H., Wei, W., Bai, X. & Chen, Z. (2016). Helium and
1321 carbon isotopes in the hot spring of Changbaishan Volcano, northeastern China: A material
1322 connection between Changbaishan Volcano and the west Pacific plate. *Journal of Volcanology*
1323 *and Geothermal Research*, 327, 398–406, doi: 10.1016/j.jvolgeores.2016.09.005
1324
1325 Wenzel, F., Lorenz, F.P., Sperner, B. & Oncescu, M.C. (1999). Seismotectonics of the Romanian
1326 Vrancea Area. In Wenzel, F., Lungu, D., Novak, O. (Eds.) *Vrancea Earthquakes: tectonics,*
1327 *hazard and risk mitigation.* (pp.15–25), Springer Netherlands
1328
1329 Werner, C., Evans, W.C., Poland, M., Tucker, D. & Doukas, M. (2009). Long-term changes in
1330 quiescent degassing at Mount Baker Volcano, Washington, USA: Evidence for a staller intrusion
1331 in 1975 and connection to a deep magma source. *Journal of Volcanology and Geothermal*
1332 *Research*, 186, 379–389, doi: 10.1016/j.jvolgeores.2009.07.006
1333
1334 Varekamp, J., Kreulen, r., Poorter, R. & Bergen, M. (1992). Carbon sources in arc volcanism,
1335 with implications for the carbon cycle. *Terra nova*, 4, 363–373, doi: 10.1111/j.1365-
1336 3121.1992.tb00825.x
1337
1338 Wortel, M.J.R. & Spakman, W. (2000). Subduction and slab detachment in the Mediterranean-
1339 Carpathian Region, *Science*, 291(5503), 10.1126/science.290.5498.1910
1340